

ebnm: An R Package for Solving the Empirical Bayes Normal Means Problem Using a Variety of Prior Families

Jason Willwerscheid
Providence College

Peter Carbonetto
University of Chicago

Matthew Stephens
University of Chicago

Abstract

The empirical Bayes normal means (EBNM) model is important to many areas of statistics, including (but not limited to) multiple testing, wavelet denoising, multiple linear regression, and matrix factorization. There are several existing software packages that can fit EBNM models under different prior assumptions and using different algorithms; however, the differences across interfaces complicate direct comparisons. Further, a number of important prior assumptions do not yet have implementations. Motivated by these issues, we developed the R package **ebnm** which provides a unified interface for efficiently fitting EBNM models using a variety of prior assumptions, including nonparametric approaches. In some cases, we incorporated existing implementations into **ebnm**; in others, we implemented new fitting procedures with a focus on speed and numerical stability. To demonstrate the capabilities of the unified interface, we compare results using different prior assumptions in two extended examples: the shrinkage estimation of baseball statistics; and the matrix factorization of genetics data (via the new R package **flashier**). In summary, **ebnm** is a convenient and comprehensive package for performing EBNM analyses under a wide range of prior assumptions.

Keywords: empirical Bayes, normal means, shrinkage estimation, mixture models, NPMLE, maximum likelihood.

1. Introduction

Given n observations x_i with known standard deviations s_i , $i = 1, \dots, n$, the normal means model (Robbins 1951; Efron and Morris 1972; Stephens 2017; Bhadra *et al.* 2019; Johnstone 2019; Sun 2020) is

$$x_i \stackrel{\text{ind.}}{\sim} \mathcal{N}(\theta_i, s_i^2), \quad (1)$$

with the unknown (true) means θ_i to be estimated. Here and throughout, we use $\mathcal{N}(\mu, \sigma^2)$ to denote the normal distribution with mean μ and variance σ^2 . The maximum-likelihood estimate of θ_i is, of course, x_i . The empirical Bayes (EB) approach to inferring θ_i attempts to improve upon the maximum-likelihood estimate by “borrowing information” across observations, exploiting the fact that each observation contains information not only about its respective mean, but also about how the means are collectively distributed (Robbins 1956; Morris 1983; Efron 2010; Stephens 2017). Specifically, the EB approach assumes that

$$\theta_i \stackrel{\text{ind.}}{\sim} g \in \mathcal{G}, \quad (2)$$

where g is a distribution to be estimated from the data, typically chosen from among some family of distributions \mathcal{G} that is specified in advance. (Note that although \mathcal{G} must be specified in advance, it can be arbitrarily flexible.)

The EB approach therefore involves fitting the model (1–2) by first using all of the observations to estimate $g \in \mathcal{G}$, then using the estimated distribution \hat{g} to compute posteriors for each mean θ_i . Commonly, g is estimated via maximum-likelihood, in which case the EB approach consists of the following:

1. Find $\hat{g} := \operatorname{argmax}_{g \in \mathcal{G}} L(g)$, where $L(g)$ denotes the marginal likelihood,

$$L(g) := p(\mathbf{x} \mid g, \mathbf{s}) = \prod_{i=1}^n \int p(x_i \mid \theta_i, s_i) g(\theta_i) d\theta_i, \quad (3)$$

and we define $\mathbf{x} := (x_1, \dots, x_n)$, $\mathbf{s} := (s_1, \dots, s_n)$.

2. Compute posterior distributions

$$p(\theta_i \mid x_i, s_i, \hat{g}) \propto \hat{g}(\theta_i) p(x_i \mid \theta_i, s_i) \quad (4)$$

and/or summaries (posterior means, variances, etc.).

We refer to this two-step process as “solving the EBNM problem.” The difficulty of both steps depends upon the choice of \mathcal{G} .

A large number of software packages have been developed to solve the EBNM problem (we review these packages below). The availability of so many methods, using a range of prior families \mathcal{G} , reflects the important role of the EBNM problem in theoretical and applied statistics. Among the many possible applications of the EBNM problem, we mention a few: wavelet denoising (Clyde and George 2000; Johnstone and Silverman 2004, 2005b); multiple testing (Efron 2010; Stephens 2017); analysis of gene expression (Love *et al.* 2014; Zhu *et al.* 2019); multiple linear regression (Kim *et al.* 2022; Mukherjee *et al.* 2023); and matrix factorization (Wang and Stephens 2021).

However, there are important gaps in the existing software. For example, as far as we are aware, no package solves the EBNM problem for one of the simplest cases: when \mathcal{G} is the set of all univariate normal distributions. Nor does any existing package implement the case where \mathcal{G} is the “point-normal” family (the family of all distributions that are a mixture of a point-mass at zero and a zero-centered normal distribution), which arises naturally when the means $\boldsymbol{\theta} = (\theta_1, \dots, \theta_n)$ are expected to be sparse. Further, each package has a different interface and outputs, which makes comparisons difficult, as well as making it difficult to develop software packages that build on EBNM methods.

Motivated by these issues, we developed the R package **ebnm**, which provides a unified interface for efficiently solving the EBNM problem using a wide variety of prior families. For some prior families, we leveraged code from existing packages, writing wrappers to match the unified **ebnm** interface; for other priors, we implemented new model-fitting algorithms with a mind toward speed and robustness. The end result is a comprehensive and user-friendly package for solving the EBNM problem.

In Section 2, we give a brief history of the EBNM problem and review existing approaches. Section 3 gives an overview of the **ebnm** package, including the unified interface and the newly

implemented prior families. In Section 4, we compare different choices of prior families and illustrate how they can impact performance. Finally, Sections 5 and 6 demonstrate usage of the `ebnm` package in two real-data applications: an analysis of weighted on-based averages for Major League Baseball players; and an exploration of EBNM-based matrix factorization methods that can identify biological patterns underlying multi-tissue gene expression data.

2. Background on the EBNM problem, and existing software

Here we review existing approaches to the EBNM problem within a common modeling framework.

2.1. Normal priors

Stein (1956) famously discovered that under quadratic loss, the maximum-likelihood estimate, $\hat{\theta}_i = x_i$, $i = 1, \dots, n$, is an inadmissible solution to the homoskedastic normal means problem

$$x_i \stackrel{\text{ind.}}{\sim} \mathcal{N}(\theta_i, s^2), \quad i = 1, \dots, n, \quad (5)$$

when $n \geq 3$. James and Stein (1961) subsequently gave an explicit formula for a shrinkage estimator that dominates the MLE. As Efron and Morris (1973) showed, a lightly modified version of the James-Stein estimator can be derived via an EB approach that assumes

$$\theta_i \stackrel{\text{ind.}}{\sim} g \in \mathcal{G}, \quad (6)$$

where the prior family \mathcal{G} is taken to be the family of zero-mean normal distributions

$$\mathcal{G}_{\text{norm0}} := \{g : g \sim \mathcal{N}(0, \sigma^2), \sigma^2 \geq 0\}. \quad (7)$$

In many applications, the mean of the θ_i 's may be non-zero, and so a natural generalization takes \mathcal{G} to be the family of normal distributions

$$\mathcal{G}_{\text{norm}} := \{g : g \sim \mathcal{N}(\mu, \sigma^2), \sigma^2 \geq 0 \text{ and } \mu \in \mathbb{R}\}. \quad (8)$$

Estimating $g \in \mathcal{G}_{\text{norm}}$ reduces to estimating σ^2 and μ . For the homoskedastic case (5), the maximum-likelihood estimates have simple, closed-form solutions:

$$\hat{\mu} = \frac{1}{n} \sum_{i=1}^n x_i, \quad (9)$$

$$\hat{\sigma}^2 = \max \left\{ 0, \frac{1}{n} \sum_{i=1}^n (x_i - \hat{\mu})^2 - s^2 \right\}. \quad (10)$$

When μ is fixed at zero, this solution is similar to the one implied by the positive-part James-Stein estimator, with the difference that it divides $\sum_{i=1}^n x_i^2$ by n rather than by $n - 2$ (Efron and Morris 1973). For the heteroskedastic case (1), the likelihood $L(\mu, \sigma^2)$ has a closed form but must be maximized numerically. In both the homoskedastic and heteroskedastic cases, the posteriors (4) are normal distributions and are available analytically. Surprisingly, we were unable to find an existing software package that handled these cases.

2.2. Other priors

Although the normal prior family has some advantages, in practice it is limiting, and so more flexible priors are usually preferred. For example, when θ may be sparse, we might like the prior to be able to capture this sparsity. One common approach is to use a “spike-and-slab” prior; that is, a mixture consisting of two components, one a point-mass at zero (the “spike”) and the other (the “slab”) belonging to some family of continuous distributions, often symmetric and centered at zero. A common choice is the “point-normal” family,

$$\mathcal{G}_{\text{pn}} := \{g : g \sim \pi_0 \delta_0 + (1 - \pi_0) \mathcal{N}(0, \sigma^2), 0 \leq \pi_0 \leq 1, \sigma^2 > 0\}. \quad (11)$$

With this choice, estimating g reduces to estimating two parameters, π_0 and σ . Similar to the normal prior, the likelihood for the point-normal has a closed form, and standard numerical optimization methods can be used to efficiently find the maximum-likelihood solution. (Since the likelihood as a function of π_0 and σ is not convex, there may be multiple “locally optimal” solutions, and typically the numerical optimization method is only guaranteed to find a locally optimal solution.) Given the estimate $\hat{g} \in \mathcal{G}_{\text{pn}}$, the posteriors (4) are mixtures of a point-mass at zero and a normal distribution, and are available analytically. Again, to our surprise, we were unable to find a software implementation of EBNM that uses the point-normal prior family, and so we have provided our own implementation in the **ebnm** package.

While a normal slab is most popular, other choices are possible. [Johnstone and Silverman \(2005b\)](#) showed that replacing the normal slab with a “heavy-tailed” distribution is guaranteed to improve accuracy. Their **EbaysThresh** software, available in R and S-PLUS ([Johnstone and Silverman 2005a](#)), implements two such priors: the point-Laplace prior,

$$\mathcal{G}_{\text{pl}} := \{g : g \sim \pi_0 \delta_0 + (1 - \pi_0) \text{Laplace}(a), 0 \leq \pi_0 \leq 1, a \geq 0\}, \quad (12)$$

and a family of priors in which the slab has “Cauchy-like” tails. Again, the optimization problem for both of these priors is non-convex, and local solutions can be found using numerical methods.

Another parametric prior that is well-suited for capturing sparse signals is the horseshoe prior ([Carvalho *et al.* 2010](#)), which models sparsity by having appreciable mass near zero rather than exactly at zero. The R package **horseshoe** ([Van der Pas *et al.* 2019](#)) includes an implementation that solves the homoskedastic EBNM problem with \mathcal{G} the family of horseshoe distributions. See [Bhadra *et al.* \(2019\)](#) for a review of other implementations of the horseshoe prior and related packages.

2.3. Nonparametric approaches

The estimate of g when \mathcal{G} is the family of *all* distributions is called the nonparametric maximum-likelihood estimate (NPML). Nonparametric approaches have been studied for nearly as long as parametric approaches ([Kiefer and Wolfowitz 1956](#); [Laird 1978](#); [Lindsay 1983](#); [Jiang and Zhang 2009](#); [Koenker and Mizera 2014](#); [Dicker and Zhao 2016](#)). In practice, most nonparametric methods approximate $\mathcal{G} = \mathcal{G}_{\text{npml}}$ by a dense but finite mixture of point masses,

$$\tilde{\mathcal{G}}_{\text{npml}} := \left\{ g : g \sim \sum_{k=1}^K \pi_k \delta_{\mu_k} \mid \pi_1, \dots, \pi_K \geq 0, \sum_{k=1}^K \pi_k = 1 \right\} \quad (13)$$

where μ_1, \dots, μ_K is a fixed, dense grid of values along the real line spanning the range of the observations. Estimating $g \in \tilde{\mathcal{G}}_{\text{npml e}}$ amounts to solving the following constrained optimization problem:

$$\begin{aligned} & \text{maximize} && \mathbf{L}\boldsymbol{\pi} \\ & \text{subject to} && \mathbf{0} \preceq \boldsymbol{\pi} \preceq \mathbf{1}_K \\ & && \boldsymbol{\pi}^T \mathbf{1}_K = 1, \end{aligned} \tag{14}$$

where $\boldsymbol{\pi} := (\pi_1, \dots, \pi_K)^T$, $\mathbf{1}_K$ is a column vector of ones of length K , and $\mathbf{L} \in \mathbb{R}^{n \times K}$ is the matrix with entries $\ell_{ik} = \mathcal{N}(x_i; \mu_k, \sigma_i^2)$. This is a convex optimization problem (Koenker and Mizera 2014); the R package **REBayes** (Koenker and Gu 2017) implements an efficient solution based on interior point optimization methods (MOSEK ApS 2019). See Kim *et al.* (2020) and Zhang *et al.* (2022) for other approaches to solving this optimization problem.

Although the fully nonparametric approach is the most flexible, the estimates of g are discrete distributions, which also leads to discrete posteriors (4) (Laird 1978). The posterior mean from a discrete prior may be perfectly adequate for point estimation even when interval estimates perform less well; see, for example, Koenker (2017). However, in some cases the lack of smoothness of the estimate can be an issue. The R package **deconvolveR** (Narasimhan and Efron 2020) uses a natural spline basis to obtain a smoothed nonparametric estimate of g . This approach can outperform the NPMLE in certain respects when the true prior is smooth (Koenker 2017).

2.4. Constrained nonparametric approaches

Constrained nonparametric approaches can also produce smoother and arguably more plausible estimates of g . For example, in the context of multiple testing, Stephens (2017) suggested that the set of all distributions that are unimodal at zero is a reasonable choice for \mathcal{G} in many settings. If it is reasonable to assume that the prior g is symmetric, one can instead take \mathcal{G} to be the family of scale mixtures of normals,

$$\mathcal{G}_{\text{smn}} := \{g : g \sim \int_0^\infty \mathcal{N}(0, \sigma^2) dh(\sigma^2) \text{ for some } h\}, \tag{15}$$

or, for slightly more flexibility, the family of all symmetric distributions that are unimodal at zero, which can be represented by scale mixtures of uniform distributions,

$$\mathcal{G}_{\text{symm-u}} := \{g : g \sim \int_0^\infty \text{Unif}[-a, a] dh(a) \text{ for some } h\}. \tag{16}$$

When these families are approximated by finite mixtures, estimating g reduces to the same convex optimization problem (14) that arises from the NPMLE, and can again be solved using fast algorithms for convex optimization. This approach is implemented in the R package **ashr** (Stephens *et al.* 2023), which, by default, uses **mixsqp** (Kim *et al.* 2020) to solve the optimization problem (14).

2.5. Flexibility of the prior families

Some prior families are more flexible than others; for example, any normal prior is also a point-normal prior, but most point-normal priors cannot be recovered as a normal prior. More broadly, we have that

$$\mathcal{G}_{\text{norm0}} \subset \mathcal{G}_{\text{pn}} \subset \mathcal{G}_{\text{smn}} \subset \mathcal{G}_{\text{symm-u}} \subset \mathcal{G}_{\text{npml e}}. \tag{17}$$

In words, the family of zero-mean normals $\mathcal{G}_{\text{norm0}}$ is a subset of the family of point-normals \mathcal{G}_{pn} , which is in turn a subset of the family of scale mixtures of normals \mathcal{G}_{smn} . \mathcal{G}_{smn} is a subset of the family of symmetric unimodal priors $\mathcal{G}_{\text{symm-u}}$, and $\mathcal{G}_{\text{symm-u}}$ is a subset of the nonparametric family of all distributions $\mathcal{G}_{\text{npml}}$. Additionally, the families of point-Laplace priors \mathcal{G}_{pl} and horseshoe priors $\mathcal{G}_{\text{horseshoe}}$ are contained in \mathcal{G}_{smn} , and $\mathcal{G}_{\text{deconvolver}} \subseteq \mathcal{G}_{\text{npml}}$.

More flexibility is in general better, but only up to a point since a prior family that is overly flexible can have the potential to “overfit” (Hastie *et al.* 2009). Ideally, one would like to select the prior family in a “data-driven” way; that is, use the data to help identify an appropriate prior family. The **ebnm** package facilitates this process by making it easy to compare prior families within a unified interface. (We caution, however, that **ebnm** does not implement formal testing.)

3. The **ebnm** package: implementation and usage

The **ebnm** package offers a unified interface for solving the EBNM problem under a wide range of prior assumptions. In addition to making available previously existing implementations via a shared interface, the package provides new implementations for several simple but useful prior families that, to our knowledge, have not previously been implemented (e.g., the normal and point-normal prior families).

3.1. The **ebnm()** function

The **ebnm()** function is the main interface to the EBNM methods. It has the following input arguments, which, apart from the first argument **x**, are all optional:

- **x**: The vector of observations, $\mathbf{x} = \{x_1, \dots, x_n\}$.
- **s**: The vector of standard errors, $\mathbf{s} = \{s_1, \dots, s_n\}$. (**s** may be a scalar for the homoskedastic case.)
- **prior_family**: The choice of prior family \mathcal{G} (see Table 1).
- **mode**: For prior families that are unimodal, this argument specifies the location of the mode. The mode may also be estimated by setting **mode** = **"estimate"**.
- **scale**: This is either the scale parameter (for parametric priors) or the grid of parameters used to approximate the nonparametric prior. By default it is **scale** = **"estimate"**, which directs **ebnm** either to estimate the scale or to automatically select the grid using grid selection strategies described in Willwerscheid (2021).
- **g_init**: An initial estimate \hat{g} which can be used to improve the search for a maximum-likelihood estimate.
- **fix_g**: When **g_init** is provided, it can also be fixed so that the posterior distributions are computed at this initial estimate.
- **output**: A character vector indicating which quantities should to be outputted.

- **optmethod**: The name of the optimization method to use. (Currently, this option is only relevant for parametric prior families.) The default choice, "nohess_nlm", is a quasi-Newton method implemented in the `nlm()` function from the **stats** package. In our tests, it worked well in most settings (see Appendix A.1). Other options include the L-BFGS-B quasi-Newton method implemented by the `optim()` function (`optmethod = "lbfgsb"`) and the trust-region method from the **trust** package (Geyer 2020) (`optmethod = "trust"`).
- **control**: A list of control parameters to be passed to the optimization function. For example, by default `nlm()` performs at most 100 iterations. To improve the quality of the fit in more challenging settings, `control = list(iterlim = 1000)` would allow `nlm()` to perform up to 1,000 iterations.

The `ebnm()` outputs include:

- **fitted_g**: The estimated prior \hat{g} .
- **log_likelihood**: The log-likelihood at \hat{g} , which can be used to compare quality of fit across different priors or prior families:

$$\log p(x_1, \dots, x_n \mid \mathbf{s}, \hat{g}) = \sum_{i=1}^n \log \int p(x_i \mid \theta_i, s_i) \hat{g}(\theta_i) d\theta_i. \quad (18)$$

- **posterior**: Summaries of the posterior distributions $p(\theta_i \mid x_i, s_i, \hat{g})$, including posterior means, posterior standard deviations and local false sign rates (Stephens 2017),

$$lfsr(i) := \min \{p(\theta_i \leq 0 \mid x_i, s_i, \hat{g}), p(\theta_i \geq 0 \mid x_i, s_i, \hat{g})\}. \quad (19)$$

- **posterior_sampler**: A function that can be used to generate random samples from the posterior distributions.

The return value is an object of class "ebnm". Many of the S3 methods that are typically associated with model fits in R also work for objects of class "ebnm", including:

- **summary()**: Gives an overview of the fitted model.
- **plot()**: Produces a scatterplot comparing the observations x_i against posterior estimates of the true means θ_i and, optionally, a visualization of the prior cumulative density function.
- **nobs()**: Returns the number of observations n used to fit the model.
- **coef()**: Returns the posterior means from the fitted model, $\hat{\theta}_i := \mathbb{E}(\theta_i \mid x_i, s_i, \hat{g})$.
- **vcov()**: Returns the posterior variances, $\text{Var}(\theta_i \mid x_i, s_i, \hat{g})$.
- **fitted()**: Returns a data frame that includes various posterior summary statistics for the unknown means θ_i such as posterior means and variances.
- **residuals()**: Returns the "residuals", which we define as the differences $x_i - \hat{\theta}_i$.
- **logLik()**: Returns the log-likelihood at \hat{g} .

- `simulate()`: Generates random draws of each θ_i from their posterior distributions.
- `confint()`: Uses the sampler to compute posterior credible intervals (more precisely, highest posterior density intervals; [Chen and Shao 1999](#)) for each θ_i .
- `quantile()`: Uses the sampler to compute posterior quantiles for each θ_i .
- `predict()`: Uses the fitted prior \hat{g} to compute posterior mean estimates $\hat{\theta}_i^{\text{new}}$ for a different set of observations x_i^{new} (with standard deviations s_i^{new}). This could be used, for example, to provide a more reliable measure of the model fit’s quality by computing the accuracy of predictions for a test set.

We will illustrate several of these methods in the examples below.

3.2. The `prior_family` argument

Table 1 gives an overview of the prior families implemented in **ebnm**. Note that some of the more specialized priors such as the “generalized binary prior” ([Liu et al. 2023](#)) are not included in this table; run `help(ebnm)` for information on these priors.

Parametric priors

Parametric priors available in **ebnm** include the normal, point-normal, point-Laplace, point-exponential and horseshoe prior families. For normal, point-normal, and point-Laplace priors, the prior mean (or mode) can either be estimated or fixed at zero. We developed special implementations for all these prior families except for the horseshoe prior, for which we relied on the **horseshoe** package ([Van der Pas et al. 2019](#)). (Note that they only implemented the horseshoe prior for the homoskedastic case.)

A closed-form solution is available only for the normal prior with homoskedastic errors, so in all other cases we use numerical methods to search for parameter estimates maximizing the likelihood. For parametric prior families, this involves searching for at most three parameters: the scale of the slab component, the mixture weight for the spike, and the mode when `mode = "estimate"`. We have found that off-the-shelf optimizers, such as `nlm()` and the `trust()` method implemented in the **trust** package ([Geyer 2020](#)), work well provided that numerical issues are avoided. For example, we found that transforming parameters to unconstrained optimization variables typically improves the optimization. We also found that analytic Hessian calculations, though available, do not consistently provide improvements in speed and quality of solution over quasi-Newton approximations to the Hessian.

The optimization method used to fit parametric priors can be controlled by the `optmethod` argument to `ebnm()`. The default optimization method for parametric priors is the Newton/quasi-Newton method `nlm()` from the **stats** package. Other available optimizers include the L-BFGS-B algorithm (via the **stats** function `optim()`) and the trust-region method from the **trust** package. In each of our experiments, `nlm()` (with the particular optimization settings we chose) was either the fastest method or differed from the fastest by less than a factor of two. Additionally, `nlm()` and `trust()` consistently converged to a solution. By contrast, `optim()` with `method = "L-BFGS-B"` occasionally diverged, or failed to find a solution, particularly in the “null” setting where the true prior was a point mass at zero (in some settings, `optim()` failed to find a solution in up to 7% of simulations). For details, see the supplementary benchmarking results in Section A.

prior_family	prior	source	support	sym?
parametric				
"normal"	$\mathcal{N}(\mu, \sigma^2)$	ebnm	\pm	yes
"point_mass"	δ_μ	ebnm		yes
"point_normal"	$\pi_0 \delta_\mu + (1 - \pi_0) \mathcal{N}(\mu, \sigma^2)$	ebnm	\pm	yes
"point_laplace"	$\pi_0 \delta_\mu + (1 - \pi_0) \text{Laplace}(\mu, a)$	ebnm	\pm	yes
"point_exponential"	$\pi_0 \delta_0 + (1 - \pi_0) \text{Exp}(a)$	ebnm	+	no
"horseshoe"	Horseshoe(τ)	horseshoe	\pm	yes
constrained nonparametric				
"normal_scale_mixture"	$\int_0^\infty \mathcal{N}(0, \sigma^2) dh(\sigma^2)$	ebnm	\pm	yes
"unimodal_symmetric"	$\int_0^\infty \text{Unif}[-a, a] dh(a)$	ashr	\pm	yes
"unimodal"	$\int_{-\infty}^\infty \text{Unif}[0, a] dh(a)$	ashr	\pm	no
"unimodal_nonnegative"	$\int_0^\infty \text{Unif}[0, a] dh(a)$	ashr	+	no
nonparametric				
"npmle"	$\int_{-\infty}^\infty \delta_x dh(x)$	ebnm	\pm	no
"deconvolver"	(Narasimhan and Efron 2020)	deconvolveR	\pm	no
other				
"flat"	$\text{Unif}(-\infty, \infty)$	ebnm	\pm	yes

Table 1: Prior families implemented in **ebnm**. The “`prior_family`” column gives the corresponding `prior_family` argument to `ebnm()`. The “source” column gives the name of the R package that implements the model fitting routines. “Support” indicates whether the prior has support for only positive realizations of θ_i (+) or all real numbers (\pm). A “yes” in the “sym?” column means that the prior is symmetric about its mode. The “flat” prior is a special case with no parameters, and recovers the maximum-likelihood estimates $\hat{\theta}_i = x_i$. It is mainly intended for use as a point of comparison with other prior families.

Constrained nonparametric priors

The constrained nonparametric families (scale mixtures of normals and unimodal, symmetric unimodal, and nonnegative unimodal families) are all implemented in package **ashr** (Stephens *et al.* 2023), and with the exception of the family of scale mixtures of normals, **ebnm** calls into these implementations to solve the EBNM problem. For scale mixtures of normals, we re-implemented the **ashr** algorithm with the aim of improving efficiency. By focusing only on this special case, we were able to reduce runtimes considerably for a number of scenarios (see Section A).

Nonparametric priors

The NPMLE can, in principle, be computed using the **ashr** implementation, but the user must specify beforehand the grid of point masses and, as with scale mixtures of normals, we

have found that **ashr** can be slow for large data sets. The **REBayes** package (Koenker and Gu 2017) was developed specifically for the NPMLE, and is typically very fast, but it relies on the commercial interior-point solver **MOSEK** (MOSEK ApS 2019). Therefore, we re-implemented the NPMLE in **ebnm** using the open source package **mixsqp** (Kim *et al.* 2020). When the number of mixture components is not too large, **mixsqp** tends to be faster than **REBayes**. However, we have found that **REBayes** can be faster than **mixsqp** when the number of mixture components is large (say, more than 100). Despite the better performance of **REBayes** in some cases, we prefer to provide a fully open-source toolkit that does not require installation of commercial software, so we have assigned **mixsqp** as the default optimization method for all nonparametric prior families.

Sign-constrained priors

In many applications, the unknown means θ_i should always be nonnegative, or always non-positive (see Section 6 for an example where means are constrained to be nonnegative). To handle such situations, we implemented two nonnegative prior families. One is a parametric prior family, the family of point-exponential distributions

$$\mathcal{G}_{\text{pe}} := \{g : g \sim \pi_0 \delta_0 + (1 - \pi_0) \text{Exp}(a), 0 \leq \pi_0 \leq 1, a \geq 0\}. \quad (20)$$

The other is the nonparametric family of nonnegative distributions that are unimodal at zero. Similar to symmetric unimodal distributions, these can be represented as mixtures of uniforms:

$$\mathcal{G}_{\text{nn}} := \{g : g \sim \int_0^\infty \text{Unif}[0, a] dh(a)\}. \quad (21)$$

Finally, for convenience, we also provide a nonpositive version of (21).

4. Numerical comparisons of prior families

To test our implementations and to compare prior families, we simulated data sets from three different data-generating distributions:

1. **Normal.** In this simplest case, we simulated from a normal prior, $\theta_i \sim \mathcal{N}(0, 2^2)$.
2. **Point- t .** In this second, more challenging scenario, the prior was both sparse and heavy-tailed, yet still symmetric: $\theta_i \sim 0.8\delta_0 + 0.2t_5(0, 1.5)$, in which $t_\nu(\mu, \sigma)$ denotes the Student- t distribution with location μ , scale σ , and ν degrees of freedom.
3. **Asymmetric Tophat.** In the third simulation scenario, we simulated data with uniformly-distributed means, $\theta_i \sim \text{Unif}[-5, 10]$. This is perhaps less realistic than the other simulations but was intended to generate data sets that are best modeled with nonparametric or constrained nonparametric priors.

In all simulations, we generated the observed means as $x_i \sim \mathcal{N}(\theta_i, 1)$.

Figure 1 summarizes results from running EBNM analyses on 10 data sets in each of the three simulation scenarios, with $n = 1,000$ observations in each data set. We used the following three measures to evaluate the EBNM model fits:

prior family	relative log-likelihood			RMSE			CI coverage		
	Normal	Point-t	Tophat	Normal	Point-t	Tophat	Normal	Point-t	Tophat
flat				1.01	1.00	0.999	0.893	0.893	0.896
normal	-4.9	-62.5	-232.9	0.900	0.663	0.978	0.893	0.923	0.897
point_normal	-4.8	-7.1	-232.9	0.900	0.531	0.978	0.892	0.871	0.895
point_laplace	-26.5	-5.5	-310.5	0.917	0.527	0.988	0.881	0.909	0.893
normal_scale_mixture	-5.3	-4.5	-239.6	0.901	0.527	0.979	0.891	0.908	0.894
unimodal_symmetric	-6.1	-4.1	-198.2	0.908	0.528	0.966	0.861	0.875	0.890
unimodal	-4.2	-1.7	-11.7	0.909	0.529	0.941	0.860	0.877	0.890
npml	0.0	0.0	0.0	0.908	0.534	0.951	0.687	0.718	0.630
deconvolver	-3.8	-18.5	-19.9	0.903	0.582	0.953	0.848	0.898	0.860
horseshoe	-161.0	-17.1	-931.8	0.987	0.532	1.10	0.812	0.903	0.826

Figure 1: Results of fitting EBNM models with different prior families to “Normal”, “Point- t ” and “Asymmetric tophat” data sets. For each prior family, the table gives the following quantities averaged across EBNM analyses of 20 data sets with $n = 1,000$ observed means: the log-likelihood at \hat{g} relative to the log-likelihood attained by the NPMLE estimate outputted by `ebnm()` with `prior_family = "npml"` (higher log-likelihoods shown with lighter shades of red are better); root mean-squared error (lower RMSEs shown with lighter shades of red are better); and the proportion of credible intervals (90% HPD inverals) containing the true mean (CI coverage values closer to 0.9 shown with lighter shades of green are better).

- The log-likelihood, which, for ease of interpretation, is shown relative to the log-likelihood attained at the NPMLE estimate. (In theory, the NPMLE estimate should always give the highest likelihood.) These log-likelihoods were obtained by calling `logLik()` on the `ebnm()` return value.
- The root mean-squared error (RMSE), which quantifies how well the estimates recover true means, and is defined as $\text{RMSE} := \sqrt{\sum_{i=1}^n (\hat{\theta}_i - \theta_i)^2 / n}$, where $\hat{\theta}_i$ denotes the posterior mean estimate, $\hat{\theta}_i := \mathbb{E}(\theta_i \mid x_i, s_i, \hat{g})$. These estimates were obtained by calling `coef()` on the `ebnm()` return value.
- The proportion of true means θ_i that are contained within the credible intervals, which we defined as 90% highest posterior density (HPD) intervals. These credible intervals were obtained by calling `confint()` on the `ebnm()` return value.

As expected, the model fit returned by `ebnm()` with `prior_family = "npml"` always attained the largest log-likelihood. More generally, log-likelihoods are expected to align with the ordering implied by the nesting of prior families (17), and indeed, this was largely the case. (Note that `deconvolveR` sometimes produces log-likelihoods that are worse than less flexible parametric models because it does not directly optimize the log-likelihood, but instead optimizes a penalized log-likelihood.) Prior families that were a poor match with the distribution used to simulate the data typically had worse log-likelihoods. For example, the

point-Laplace and horseshoe families had difficulty matching the shape of the normal distribution. In the Asymmetric Tophat simulation scenario, all symmetric priors performed poorly by the log-likelihood measure.

The RMSE evaluates the quality of the posterior estimates $\hat{\theta}_i$ generated by an EBNM analysis (a lower RMSE is better). As a baseline measure, we computed posterior estimates from the EBNM model with a “flat” prior, which effectively gives us maximum-likelihood estimates $\hat{\theta}_i = x_i$. Reassuringly, nearly all prior families improved upon the maximum-likelihood estimates, although the improvement was sometimes small, particularly when the prior family was a poor match with the true distribution (e.g., symmetric prior families in the Asymmetric Tophat scenario). The horseshoe family is best suited for “sparse” settings — in which many or most θ_i are zero — and so it was not unexpected that it performed poorly in the Normal and Asymmetric Tophat settings. On the contrary, **deconvolveR** is best suited for non-sparse settings, which explains its poor performance on the Point- t data sets. Overall, higher log-likelihoods were indicative of better accuracy in estimates of θ_i , except when the model overfitted; so for example the NPMLE tended to achieve a better log-likelihood than the unimodal prior in the Asymmetric Tophat scenario, but its accuracy (RMSE) was worse, presumably because of the greater tendency of the NPMLE to overfit.

The “CI coverage” measures how well the credible intervals are calibrated. A known limitation of empirical Bayes methods is that they often underestimate uncertainty in the posteriors (since uncertainty in the estimate of g is not taken into account). Indeed, the HPD intervals tended to be too small (i.e., less than 90%) for most prior families and simulation scenarios (Figure 1). Still, in most cases the intervals were not far off the target coverage of 90%, showing that the CI intervals are surprisingly robust to modeling assumptions. The lone exception was the NPMLE, which tended to have much poorer coverage because, as noted above, it results in a discrete prior that can greatly underestimate uncertainty.

Finally, to assess the ability of our implementation to handle large data sets, we recorded runtimes for simulated (Point- t) data sets ranging in size from $n = 200$ to $n = 1,000,000$. These analyses were performed in R 4.2.2 on a desktop running Windows 11 Pro with an Intel Core i9-13900KF multicore processor and 32 GB of memory. Results are summarized in Figure 2. As expected, the less flexible priors with the fewest parameters tended to also be the fastest, whereas the most complex methods (e.g., unimodal prior, NPMLE) were slower than the fastest methods by several orders of magnitude. Most importantly, all prior families implemented in **ebnm** scaled well to large data sets; the computational effort grew linearly or close to linearly in n .

5. Analyzing weighted on-base averages of MLB players

A longstanding tradition in empirical Bayes research is to include an analysis of batting averages using data from Major League Baseball (see, for example, [Brown 2008](#); [Jiang and Zhang 2010](#); [Gu and Koenker 2017](#)). Until recently, batting averages were the most important measurement of a hitter’s performance, with the prestigious yearly “batting title” going to the hitter with the highest average. However, with the rise of baseball analytics, metrics that better correlate to teams’ overall run production have become increasingly preferred. One such metric is wOBA (“weighted on-base average”), which is both an excellent measure of a hitter’s offensive production and, unlike competing metrics such as MLB’s xwOBA ([Sharpe](#)

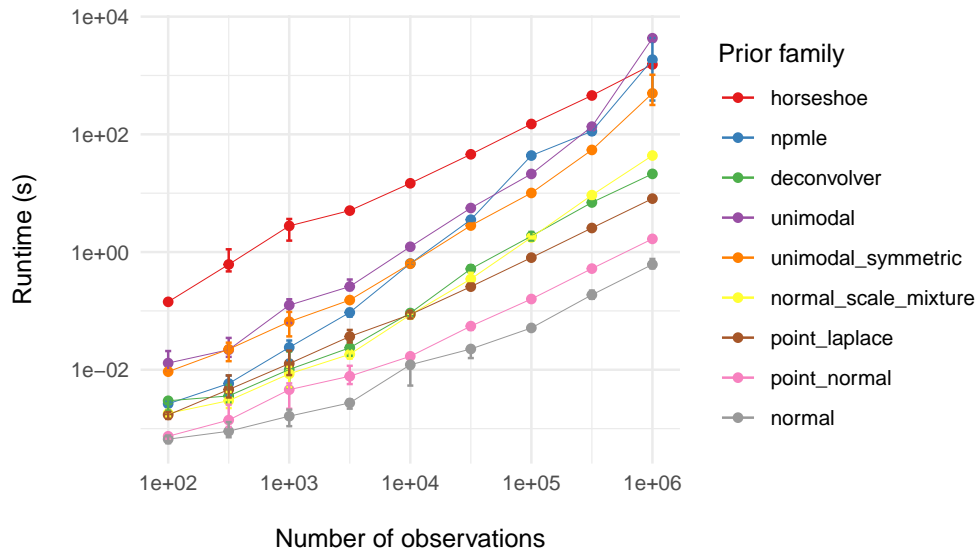


Figure 2: Runtimes for fitting EBNM models with different prior families to data sets ranging in size from $n = 100$ to $n = 1,000,000$. For each combination of sample size (n) and prior family, an EBNM model was fit to 20 data sets simulated using the Point- t distribution. Each point in the plot gives the average runtime over all 20 simulations; the error bars depict 10% and 90% quantiles.

2019) or Baseball Prospectus’s DRC+ (Judge 2019), can be calculated using publicly available data and methods.

Initially proposed by Tango *et al.* (2006), wOBA assigns values (“weights”) to hitting outcomes according to how much the outcome contributes on average to run production. For example, while batting average treats singles identically to home runs, wOBA gives a hitter more than twice as much credit for a home run.¹

Given a vector of wOBA weights \mathbf{w} , hitter i ’s wOBA is the weighted average

$$x_i := \mathbf{w}^T \mathbf{z}^{(i)} / n_i, \quad (22)$$

where $\mathbf{z}^{(i)} = (z_1^{(i)}, \dots, z_7^{(i)})$ tallies outcomes (singles, doubles, triples, home runs, walks, hit-by-pitches, and outs) over the hitter’s n_i plate appearances (PAs). Modeling hitting outcomes as i.i.d.

$$\mathbf{z}^{(i)} \sim \text{Multinomial}(n_i, \boldsymbol{\pi}^{(i)}), \quad (23)$$

where $\boldsymbol{\pi}^{(i)} = (\pi_1, \dots, \pi_7)$ is the vector of “true” outcome probabilities for hitter i , we can regard x_i as a point estimate for the hitter’s “true wOBA skill”

$$\theta_i := \mathbf{w}^T \boldsymbol{\pi}^{(i)}. \quad (24)$$

Standard errors for the x_i ’s can be estimated as

$$s_i^2 = \mathbf{w}^T \hat{\boldsymbol{\Sigma}}^{(i)} \mathbf{w} / n_i, \quad (25)$$

¹Weights are updated from year to year, but wOBA weights for singles have remained near 0.9 for the last several decades, while weights for home runs have hovered around 2.0 (FanGraphs 2023).

where $\hat{\Sigma}^{(i)}$ is the estimate of the covariance matrix for the multinomial model (23) obtained by setting $\boldsymbol{\pi} = \hat{\boldsymbol{\pi}}$,² where

$$\hat{\boldsymbol{\pi}}^{(i)} = \mathbf{z}^{(i)}/n_i. \quad (26)$$

The relative complexity of wOBA makes it well suited for analysis via **ebnm**. With batting average, a common approach is to obtain empirical Bayes estimates using a beta-binomial model (see, for example, Robinson 2017). With wOBA, one can estimate hitting outcome probabilities by way of a Dirichlet-multinomial model; alternatively, one can approximate the likelihood as normal and fit an EBNM model directly to the observed wOBAs. In the following, we take the latter approach.

We begin by loading and inspecting the wOBA data set, which consists of wOBAs and standard errors for the 2022 MLB regular season:

```
R> library(ebnm)
R> data(wOBA)
R> nrow(wOBA)
```

```
[1] 688
```

```
R> head(wOBA)
```

	FanGraphsID	Name	Team	PA	x	s
1	19952	Khalil Lee	NYM	2	1.036	0.733
2	16953	Chadwick Tromp	ATL	4	0.852	0.258
3	19608	Otto Lopez	TOR	10	0.599	0.162
4	24770	James Outman	LAD	16	0.584	0.151
5	8090	Matt Carpenter	NYY	154	0.472	0.054
6	15640	Aaron Judge	NYY	696	0.458	0.024

Column “x” contains each player’s wOBA for the 2022 season, which we regard as an estimate of the player’s “true” wOBA skill. Column “s” provides standard errors.

Next, we visualize the overall distribution of wOBAs:

```
R> library(ggplot2)
R> ggplot(wOBA, aes(x = x)) +
+   geom_histogram(bins = 64, color = "black") +
+   theme_classic()
```

As the histogram (Figure 3) shows, most players finished the season with a wOBA between .200 and .400.³ A few had very high wOBAs (>.500), while others had wOBAs at or near zero. A casual inspection of the data suggests that players with these very high (or very low) wOBAs were simply lucky (or unlucky). For example, the 4 players with the highest wOBAs

²To deal with small sample sizes, we conservatively lower bound each standard error by the standard error that would be obtained by plugging in league-average event probabilities $\hat{\boldsymbol{\pi}}_{\text{lg}} = \sum_{i=1}^N \mathbf{z}^{(i)} / \sum_{i=1}^N n_i$, where N is the number of hitters in the data set.

³Throughout, we follow the convention of reporting wOBAs using three decimal places.

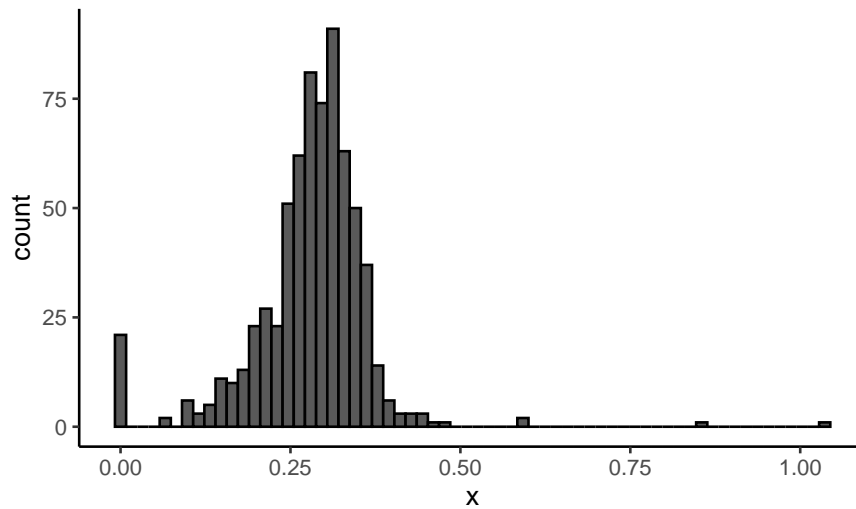


Figure 3: Histogram of MLB player wOBAs from the 2022 season.

each had fewer than 16 PAs. It is very unlikely that they would have sustained this high level of production over a full season’s worth of PAs.

In contrast, Aaron Judge’s production — which included a record-breaking number of home runs — appears to be “real,” since it was sustained over nearly 700 PAs. Other cases are more ambiguous: how, for example, are we to assess Matt Carpenter, who had several exceptional seasons between 2013 and 2018 but whose output steeply declined in 2019–2021 before his surprising “comeback” in 2022? An empirical Bayes analysis can help to answer this and other questions.

Function `ebnm()` is the main interface for fitting the empirical Bayes normal means model (1)–(2); it is a “Swiss army knife” that allows for various choices of prior family \mathcal{G} as well as providing multiple options for fitting and tuning models. For example, we can fit a normal means model with the prior family \mathcal{G} taken to be the family of normal distributions as follows:

```
R> x <- wOBA$x
R> s <- wOBA$s
R> names(x) <- wOBA$Name
R> names(s) <- wOBA$Name
R> fit_normal <- ebnm(x, s, prior_family = "normal", mode = "estimate")
```

(The default behavior is to fix the prior mode at zero. Since we certainly do not expect the distribution of true wOBA skill to have a mode at zero, we set `mode = "estimate"`.)

We note in passing that the `ebnm` package has a second model-fitting interface, in which each prior family gets its own function:

```
R> fit_normal <- ebnm_normal(x, s, mode = "estimate")
```

Textual and graphical overviews of results can be obtained using, respectively, methods `summary()` and `plot()`. The summary method appears as follows:

```
R> summary(fit_normal)
```

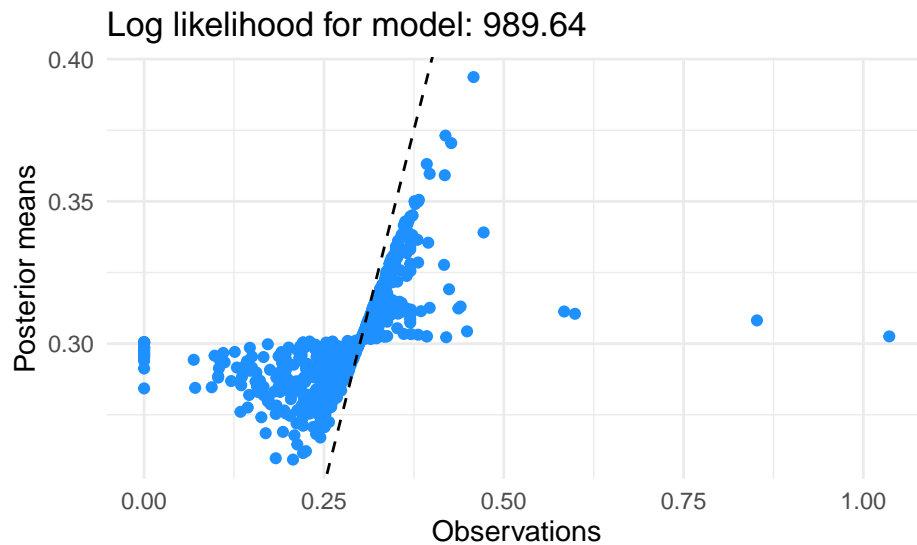


Figure 4: Initial wOBA estimates (“observations”) vs. posterior mean wOBA estimates, in which the posterior estimates were obtained by fitting a prior from the family of normal distributions. The dashed line shows the diagonal $x = y$.

Call:

```
ebnm_normal(x = x, s = s, mode = "estimate")
```

EBNM model was fitted to 688 observations with `_heteroskedastic_` standard errors.

The fitted prior belongs to the `_normal_` prior family.

2 degrees of freedom were used to estimate the model.

The log likelihood is 989.64.

Available posterior summaries: `_mean_`, `_sd_`.

Use method `fitted()` to access available summaries.

A posterior sampler is `_not_` available.

One can be added via function `ebnm_add_sampler()`.

The `plot()` method visualizes results, comparing the “observed” values x_i (the initial wOBA estimates) against the empirical Bayes posterior mean estimates $\hat{\theta}_i$:

```
R> plot(fit_normal)
```

See Figure 4 for this plot. Shrinkage effects are clearly visible, with the most extreme wOBAs on either end of the spectrum being strongly shrunk toward the league average (around .300). Since `plot()` returns a “ggplot” object (Wickham 2016), the plot can conveniently be customized using **ggplot2** syntax. For example, one can vary the color of the points by the number of plate appearances:

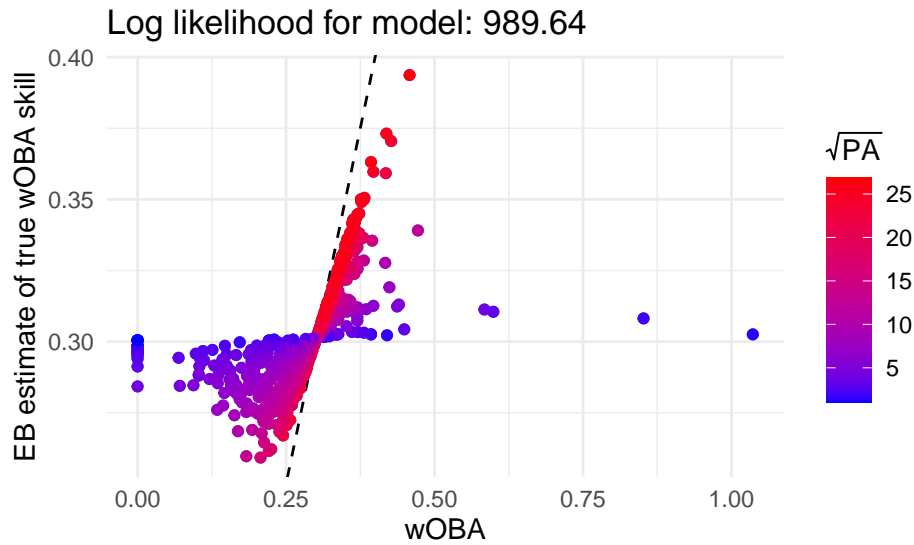


Figure 5: The same as Figure 4, except that the color of the points is varied by the number of plate appearances. The dashed line shows the diagonal ($x = y$) line.

```
R> plot(fit_normal) +
+   geom_point(aes(color = sqrt(wOBA$PA))) +
+   labs(x = "wOBA", y = "EB estimate of true wOBA skill",
+        color = expression(sqrt(PA))) +
+   scale_color_gradient(low = "blue", high = "red")
```

See Figure 5 for this customized plot. By varying the color of points, we see that the wOBA estimates with higher standard errors or fewer plate appearances (blue points) tend to be shrunk toward the league average much more strongly than wOBAs from hitters with many plate appearances (red points).

Above, we used `head()` to view data for the first 6 hitters in the data set. Let's now see what the EBNM analysis suggests might be their "true" wOBA skill. We use the `fitted()` method, which returns a posterior summary for each hitter:⁴

```
> print(head(fitted(fit_normal)), digits = 3)
```

	mean	sd
Khalil Lee	0.303	0.0287
Chadwick Tromp	0.308	0.0286
Otto Lopez	0.310	0.0283
James Outman	0.311	0.0282
Matt Carpenter	0.339	0.0254
Aaron Judge	0.394	0.0184

The wOBA estimates of the first four ballplayers are shrunk strongly toward the league

⁴By default, `fitted()` returns a posterior mean and posterior standard deviation, but other posterior information can be returned, including the *local false sign rate* (Stephens 2017).

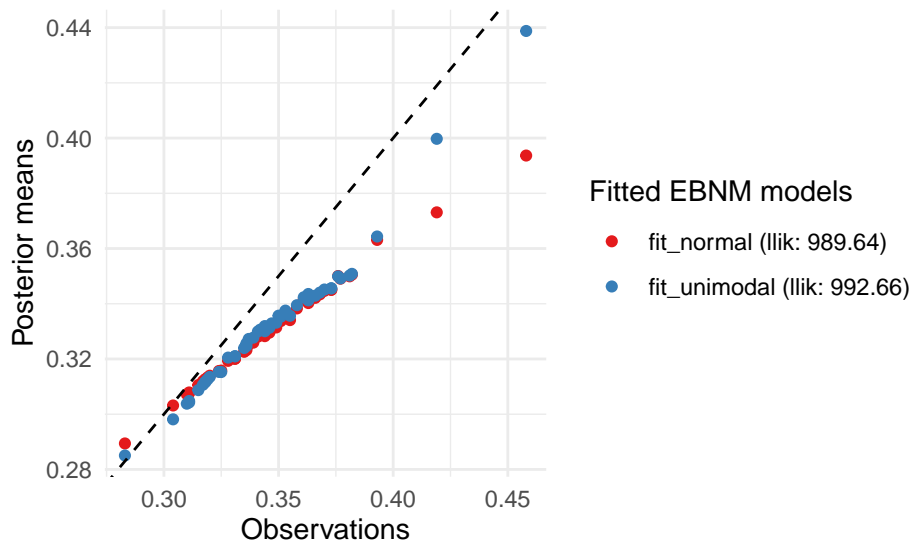


Figure 6: Initial wOBA estimates (“Observations”) vs. posterior mean wOBA estimates, in which the posterior estimates were obtained by fitting a prior from the family of normal distributions (`prior_family = "normal"`) and the family of unimodal distributions (`prior_family = "unimodal"`). Results are shown only for the top 50 ballplayers by number of plate appearances.

average, reflecting the fact that these players had very few plate appearances (and indeed, we were not swayed by their very high initial wOBA estimates).

Carpenter had many more plate appearances (154) than these other four players, but according to this model we should remain skeptical about his strong performance; after factoring in the prior, we judge his “true” performance to be much closer to the league average, downgrading an initial estimate of .472 to the final posterior mean estimate of .339.

Judge’s “true” wOBA is also estimated to be much lower (.394) than the initial estimate (.458) despite sustaining this high level of production over a full season (696 PAs). For this reason, one might ask whether a prior that is more flexible than the normal prior—that is, a prior that can better adapt to “outliers” like Judge—might produce a different result. The **ebnm** package is very well suited to answering this question. For example, to obtain results using a “unimodal” prior instead of a normal prior, we need only change `prior_family` from “normal” to “unimodal”:

```
R> fit_unimodal <- ebnm(x, s, prior_family = "unimodal", mode = "estimate")
```

It is straightforward to produce a side-by-side visualization of the fitted models simply by including both models as arguments to the `plot()` method:

```
top50 <- order(wOBA$PA, decreasing = TRUE)
top50 <- top50[1:50]
plot(fit_normal, fit_unimodal, subset = top50)
```

We also used the `subset` argument to focus on the results for Judge and other players with the most plate appearances. The plot resulting from this call is shown in Figure 6. Indeed, this

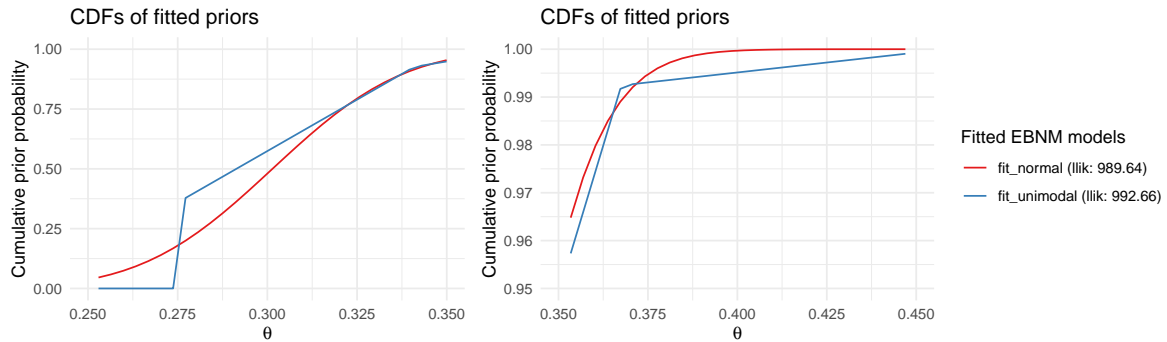


Figure 7: The cumulative distribution functions (CDFs) for the priors that were fitted to the 2022 MLB wOBA data: the normal prior (`prior_family = "normal"`) and the unimodal prior (`prior_family = "unimodal"`). The right-hand panel shows the right tail of the priors in more detail.

plot illustrates the ability of the unimodal prior to better adapt to the data: wOBA estimates for players with a lot of plate appearances are not adjusted quite so strongly toward the league average. To compare in more detail, we see for example that Judge’s wOBA estimate from the model with the unimodal prior (the `"mean2"` column) remains much closer to the original wOBA estimate:

```
R> dat <- cbind(wOBA[, c("PA", "x")],
+             fitted(fit_normal),
+             fitted(fit_unimodal))
R> names(dat) <- c("PA", "x", "mean1", "sd1", "mean2", "sd2")
R> print(head(dat), digits = 3)
```

	PA	x	mean1	sd1	mean2	sd2
Khalil Lee	2	1.036	0.303	0.0287	0.302	0.0277
Chadwick Tromp	4	0.852	0.308	0.0286	0.307	0.0306
Otto Lopez	10	0.599	0.310	0.0283	0.310	0.0315
James Outman	16	0.584	0.311	0.0282	0.311	0.0318
Matt Carpenter	154	0.472	0.339	0.0254	0.355	0.0430
Aaron Judge	696	0.458	0.394	0.0184	0.439	0.0155

Carpenter’s wOBA estimate is also higher under the more flexible unimodal prior, but is still adjusted much more than Judge’s in light of Carpenter’s smaller sample size. It is also interesting that the unimodal prior assigns greater uncertainty (the `"sd2"` column) to this estimate compared to the normal prior.

Recall that the two normal means models differ only in the priors used, so we can understand the differences in the shrinkage behavior of these models by inspecting the priors. Calling `plot()` with `incl_cdf = TRUE` shows the cumulative distribution functions (CDFs) of the fitted priors \hat{g} . Since we are particularly interested in understanding the differences in shrinkage behaviour for the largest wOBAs such as Judge’s, we create a second plot that zooms in on wOBAs over .350:

```
R> plot(fit_normal, fit_unimodal, incl_cdf = TRUE, incl_pm = FALSE) +
+   xlim(c(0.250, 0.450)) +
+   guides(color = "none")
R> plot(fit_normal, fit_unimodal, incl_cdf = TRUE, incl_pm = FALSE) +
+   xlim(c(0.350, 0.450)) +
+   ylim(c(0.95, 1))
```

These plots are shown in Figure 7. The plot on the right shows that the fitted normal prior has almost no mass on wOBAs above .400, explaining why Judge’s wOBA estimate is shrunk so strongly toward the league average, whereas the unimodal prior is flexible enough to permit larger posterior estimates above .400.

The posterior means and standard errors returned from the `ebnm()` call cannot be used to obtain credible intervals (except for the special case of the normal prior). Therefore, we provide additional methods `confint()` and `quantile()` which return, respectively, credible intervals (or more precisely, *highest posterior density* intervals: Box and Tiao 1965; Chen and Shao 1999) and posterior quantiles for each observation. These are implemented using Monte Carlo techniques, which can be slow for large data sets, so credible intervals are not computed by default. The following code computes 80% highest posterior density (HPD) intervals for the EBNM model with unimodal prior. (We add a Monte Carlo sampler using function `ebnm_add_sampler()`; alternatively, we could have added a sampler in our initial calls to `ebnm()` by specifying `output = output_all()`.) We set a seed for reproducibility:

```
R> fit_unimodal <- ebnm_add_sampler(fit_unimodal)
R> set.seed(1)
R> print(head(confint(fit_unimodal, level = 0.8)), digits = 3)
```

	CI.lower	CI.upper
Khalil Lee	0.277	0.328
Chadwick Tromp	0.277	0.334
Otto Lopez	0.277	0.336
James Outman	0.277	0.335
Matt Carpenter	0.277	0.389
Aaron Judge	0.428	0.458

Interestingly, the 80% credible interval for Carpenter is very wide, and shares the same lower bound as the first four ballplayers with very few plate appearances.

5.1. Reanalyzing the baseball data using a nonparametric prior

Above, we demonstrated how the `ebnm` package makes it is easy to perform EBNM analyses with different types of priors, then compare results across different prior choices. Each prior family makes different assumptions about the data which, *a priori*, may be more or less plausible. An alternative to prior families that make specific assumptions about the data is to use the prior family that contains *all* distributions $\mathcal{G}_{\text{npml}}$, which is in a sense “assumption free” (see Section 2 for background). Here we re-analyze the wOBA data set to illustrate the use of this prior family. Note that although nonparametric priors require specialized computational techniques, switching to a nonparametric prior is seamless in `ebnm`, as these

implementation details are hidden. Similar to above, we need only make a single change to the `prior_family` argument:

```
R> fit_npmlle <- ebnm(x, s, prior_family = "npmlle")
```

(Note that because the family $\mathcal{G}_{\text{npmlle}}$ is not unimodal, the `mode = "estimate"` option is not relevant here.)

Although the implementation details are hidden by default, it can sometimes be helpful to see what is going on “behind the scenes,” particularly for flagging or diagnosing issues. By default, `ebnm` uses the `mixsqp` package (Kim *et al.* 2020) to fit the NPMLE $\hat{g} \in \mathcal{G}_{\text{npmlle}}$. We can monitor convergence of the mix-SQP optimization algorithm by setting the `verbose` control argument to `TRUE`:

```
R> fit_npmlle <- ebnm(x, s, prior_family = "npmlle",
+                   control = list(verbose = TRUE))
```

```
Running mix-SQP algorithm 0.3-48 on 688 x 95 matrix
```

```
convergence tol. (SQP):      1.0e-08
conv. tol. (active-set):    1.0e-10
zero threshold (solution):  1.0e-08
zero thresh. (search dir.): 1.0e-14
l.s. sufficient decrease:   1.0e-02
step size reduction factor: 7.5e-01
minimum step size:         1.0e-08
max. iter (SQP):           1000
max. iter (active-set):     20
number of EM iterations:    10
```

```
Computing SVD of 688 x 95 matrix.
```

```
Matrix is not low-rank; falling back to full matrix.
```

iter	objective	max(rdual)	nnz	stepsize	max.diff	nqp	nls
1	+9.583407733e-01	-- EM --	95	1.00e+00	6.08e-02	--	--
2	+8.298700300e-01	-- EM --	95	1.00e+00	2.87e-02	--	--
3	+7.955308369e-01	-- EM --	95	1.00e+00	1.60e-02	--	--
4	+7.819858634e-01	-- EM --	68	1.00e+00	1.05e-02	--	--
5	+7.753787534e-01	-- EM --	53	1.00e+00	7.57e-03	--	--
6	+7.717040208e-01	-- EM --	49	1.00e+00	5.73e-03	--	--
7	+7.694760705e-01	-- EM --	47	1.00e+00	4.48e-03	--	--
8	+7.680398878e-01	-- EM --	47	1.00e+00	3.58e-03	--	--
9	+7.670690681e-01	-- EM --	44	1.00e+00	2.91e-03	--	--
10	+7.663865515e-01	-- EM --	42	1.00e+00	2.40e-03	--	--
1	+7.658902386e-01	+6.493e-02	39	-----	-----	--	--
2	+7.655114904e-01	+5.285e-02	19	1.00e+00	9.88e-02	20	1
3	+7.627839841e-01	+1.411e-02	7	1.00e+00	1.28e-01	20	1
4	+7.626270875e-01	+2.494e-04	7	1.00e+00	3.23e-01	8	1
5	+7.626270755e-01	+1.748e-08	7	1.00e+00	4.94e-04	2	1
6	+7.626270755e-01	-2.796e-08	7	1.00e+00	2.76e-07	2	1

```
Optimization took 0.03 seconds.
```

```
Convergence criteria met---optimal solution found.
```

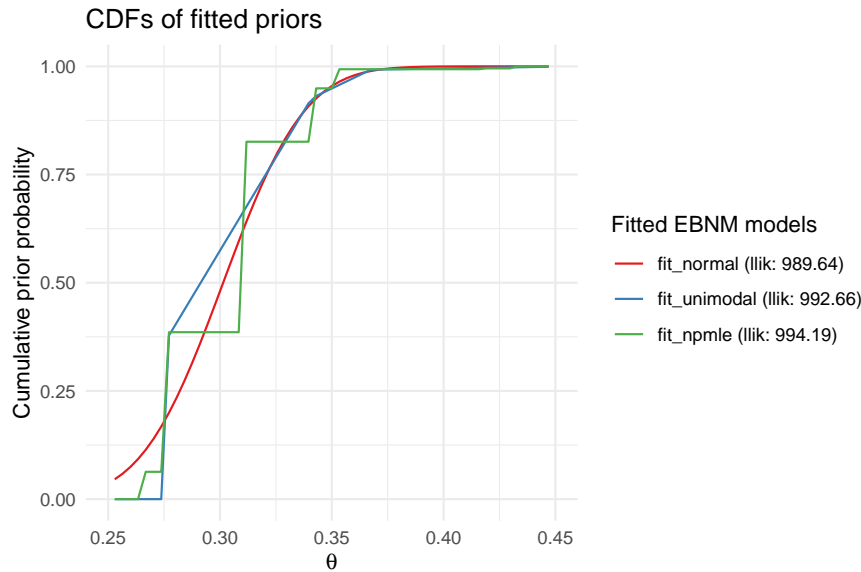


Figure 8: The CDFs for priors fitted to the 2022 MLB wOBA data: the normal prior (`prior_family = "normal"`), the unimodal prior (`prior_family = "unimodal"`), and the NPMLE (`prior_family = "npml"`).

This output shows no issues with convergence of the optimization algorithm; the mix-SQP algorithm converged to the solution (up to numerical rounding error) in only 6 iterations. In some cases, convergence issues can arise when fitting nonparametric models to large or complex data sets, and revealing the details of the optimization can help to pinpoint these issues.

Next, we visually compare the three fits obtained so far:

```
plot(fit_normal, fit_unimodal, fit_npml, incl_cdf = TRUE, subset = top50)
```

The plots generated by this call are shown in Figures 8 and 9. As before, estimates largely agree, differing primarily at the tails. Both the unimodal prior family and the NPMLE are sufficiently flexible to avoid the strong shrinkage behavior of the normal prior family.

Fits can be compared quantitatively using the `logLik()` method, which, in addition to the log likelihood for each model, usefully reports the number of free parameters (i.e., degrees of freedom):

```
R> logLik(fit_unimodal)
'log Lik.' 992.6578 (df=40)
```

```
R> logLik(fit_npml)
'log Lik.' 994.193 (df=94)
```

A nonparametric prior \mathcal{G} is approximated by K mixture components on a fixed grid, with the mixture proportions to be estimated (see Section 2). We can infer from the above output that

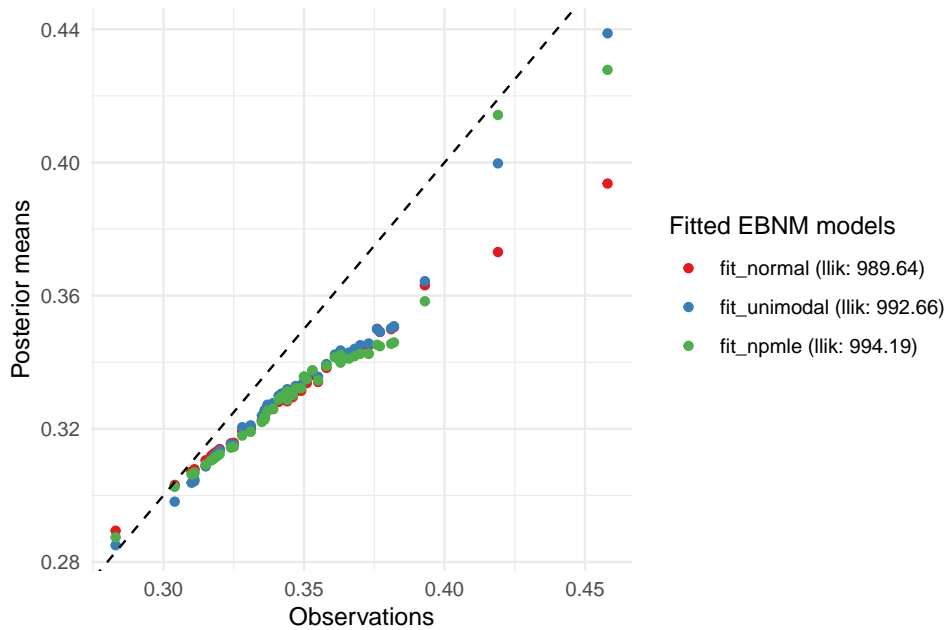


Figure 9: Initial wOBA estimates (“Observations”) vs. posterior mean wOBA estimates for priors fitted to the 2022 MLB wOBA data: the normal prior (`prior_family = "normal"`), the unimodal prior (`prior_family = "unimodal"`), and the NPMLE (`prior_family = "npmlle"`). Results are shown only for the top 50 ballplayers by number of plate appearances.

$\mathcal{G}_{\text{npmlle}}$ has been approximated as a family of mixtures over a grid of $K = 95$ point masses spanning the range of the data. (The number of degrees of freedom is one fewer than K because the mixture proportions must always sum to 1, which removes one degree of freedom from the estimation of $\boldsymbol{\pi}$.)

The default behaviour for nonparametric prior families is to choose K such that the likelihood obtained using estimate \hat{g} should be (on average) within one log-likelihood unit of the optimal estimate from among the entire nonparametric family \mathcal{G} (that is, provided that the “true” prior is $g \in \mathcal{G}$; see Willwerscheid 2021). Thus, a finer approximating grid should not yield a large improvement in the log-likelihood. We can check this by using `ebnm_scale_npmlle()` to create a finer grid:

```
R> scale_npmlle <- ebnm_scale_npmlle(x, s, KLdiv_target = 0.001/length(x),
+                                   max_K = 1000)
R> fit_npmlle_finer <- ebnm_npmlle(x, s, scale = scale_npmlle)
R> logLik(fit_npmlle)

'log Lik.' 994.193 (df=94)

R> logLik(fit_npmlle_finer)

'log Lik.' 994.2502 (df=528)
```

As the theory predicts, a much finer grid, with $K = 529$, results in only a modest improvement in the log-likelihood. **ebnm** provides similar functions to customize grids for unimodal and normal scale mixture prior families.

One potential issue with the NPMLE is that, since it is discrete (as the CDF plot in Figure 8 makes apparent), observations are variously shrunk toward one of the support points, which can result in poor interval estimates. For illustration, we calculate 10% and 90% quantiles:

```
R> fit_npmlle <- ebnm_add_sampler(fit_npmlle)
R> print(head(quantile(fit_npmlle, probs = c(0.1, 0.9))), digits = 3)
```

	10%	90%
Khalil Lee	0.276	0.342
Chadwick Tromp	0.276	0.342
Otto Lopez	0.276	0.342
James Outman	0.276	0.342
Matt Carpenter	0.309	0.430
Aaron Judge	0.419	0.430

Each credible interval bound is constrained to lie at one of the support points of the NPMLE \hat{g} . The interval estimate for Judge strikes us as far too narrow. Indeed, the NPMLE can sometimes yield degenerate interval estimates:

```
R> confint(fit_npmlle, level = 0.8, parm = "Aaron Judge")
```

	CI.lower	CI.upper
Aaron Judge	0.4298298	0.4298298

To address this issue, the **deconvolveR** package (Narasimhan and Efron 2020) uses a penalized likelihood that encourages “smooth” priors \hat{g} ; that is, priors \hat{g} for which few of the mixture proportions are zero:

```
R> fit_deconv <- ebnm_deconvolver(x / s, output = ebnm_output_all())
R> plot(fit_npmlle, fit_deconv, incl_cdf = TRUE, incl_pm = FALSE)
```

See Figure 10 for results; in particular, note that the estimated prior \hat{g} is in fact much “smoother” than the NPMLE prior.

Note however that the “true” means θ being estimated are z -scores rather than raw wOBA skill, as package **deconvolveR** fits a model to z -scores rather than observations and associated standard errors. While this is reasonable in many settings, it does not seem appropriate for the present analysis:

```
R> print(head(quantile(fit_deconv, probs = c(0.1, 0.9)) * s), digits = 3)
```

	10%	90%
Khalil Lee	0.400	2.000
Chadwick Tromp	0.563	1.127
Otto Lopez	0.354	0.796

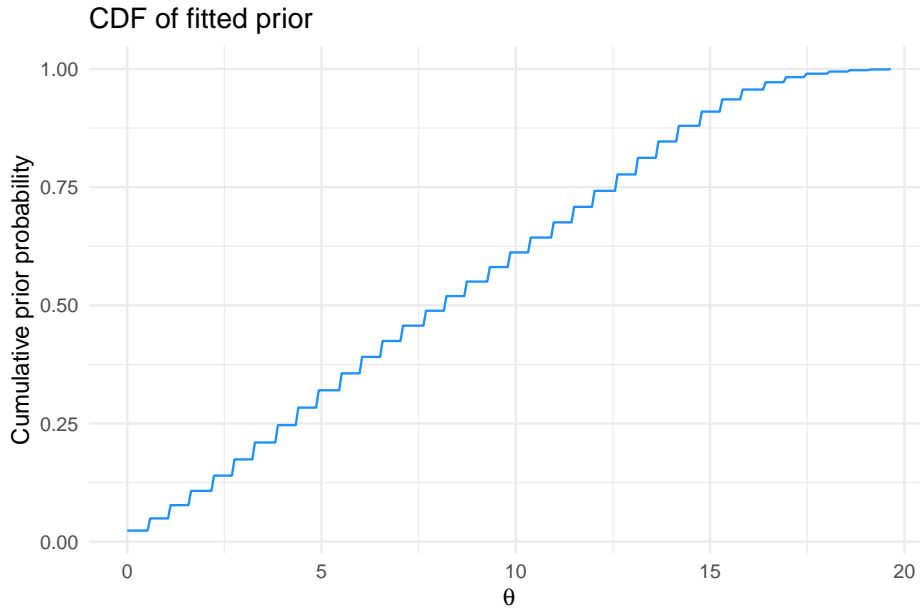


Figure 10: The CDF for the prior fitted to 2022 MLB wOBA data using **deconvolveR** (Narasimhan and Efron 2020).

James Outman	0.412	0.742
Matt Carpenter	0.413	0.531
Aaron Judge	0.406	0.459

These interval estimates do not match our basic intuitions; for example, a wOBA over .600 has never been sustained over a full season.

6. Flexible empirical Bayes matrix factorization via **ebnm**

In our next example, we illustrate the use of the **ebnm** package for the more challenging problem of *matrix factorization*. In particular, we illustrate the matrix factorization methods implemented in the R package **flashier** (Willwerscheid 2021; Willwerscheid *et al.* 2023). Although we do not directly call **ebnm** functions, the **flashier** interface and implementation borrow heavily from **ebnm**, so this example serves to apply **ebnm** to a larger and more challenging statistical problem.

The matrix we analyze in this example is a $1,000 \times 44$ matrix of z -scores quantifying support for association between genetic variants in the human genome (the rows of the matrix) and gene expression measured across 44 human tissues (the columns):

```
R> library(flashier)
R> data(gtex)
R> nrow(gtex)
```

```
[1] 1000
```

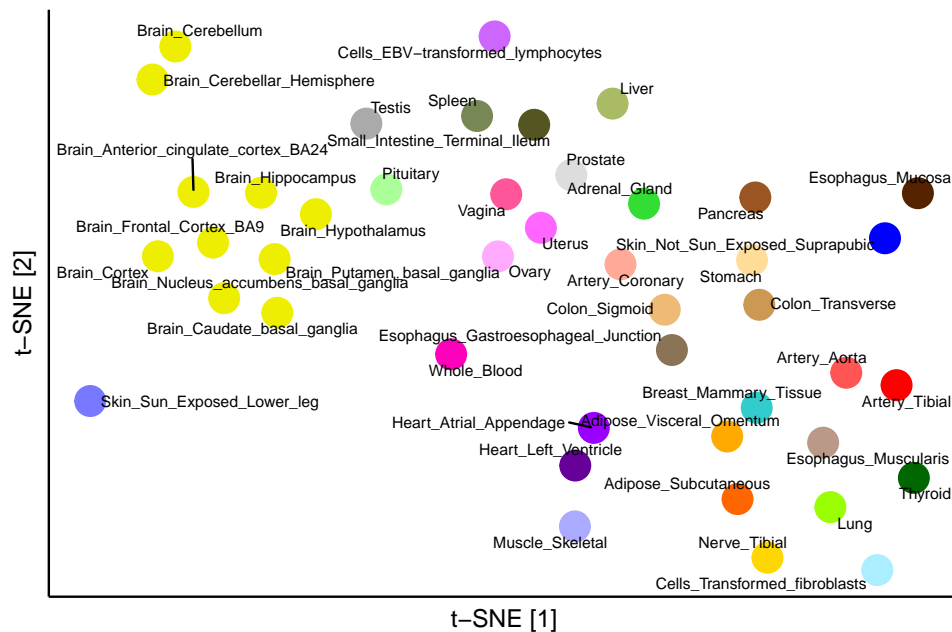


Figure 11: 2-d t -SNE of the 44 GTEx tissues. We use the same color palette as Wang and Stephens (2021) (object `gtex_colors` in `flashier`), which was designed to link similar tissues together visually: For example, brain tissues are all bright yellow; arterial tissues are pink to red; heart tissues are shades of purple; and skin tissues are blue.

```
R> ncol(gtex)
```

```
[1] 44
```

```
R> gtex[1:2,1:2]
```

	Adipose_Subcutaneous	Adipose_Visceral_Omentum
ENSG00000099977.9_22_24266954_A_C_b37	8.099352	6.4129683
ENSG00000233868.1_2_222475922_A_G_b37	1.079264	-0.7760486

The genetic variants are linked to genes, so each row of the matrix corresponds to a gene (the names of the rows are the genes' Ensembl ids). These z -scores were originally calculated in Urbut *et al.* (2019) using data made available from the Genotype Tissue Expression (GTEx) project (Lonsdale *et al.* 2013), so we refer to this as the “GTEx data set.”

Our motivation for factorizing the GTEx data matrix is to identify patterns (“factors”) that give insight into the genetics of the 44 tissues: in particular, which tissues tend to act in concert, and to what degree? First, to get some intuition into the structure of this data set, we visualize the tissues in a 2-d embedding generated by t -SNE (Van der Maaten and Hinton 2008; Van der Maaten 2014; Krijthe 2015):

```
R> library(Rtsne)
R> library(ggrepel)
```

```

R> set.seed(1)
R> out <- Rtsne(t(gtex), dims = 2, perplexity = 10)
R> pdat <- data.frame(d1 = out$Y[, 1],
+                   d2 = out$Y[, 2],
+                   tissue = colnames(gtex))
R> ggplot(pdat, aes(x = d1, y = d2, label = tissue)) +
+   geom_point(size = 6, color = gtex_colors) +
+   geom_text_repel(size = 2.5, max.overlaps = Inf) +
+   labs(x = "t-SNE [1]", y = "t-SNE [2]") +
+   theme_classic()
+   theme(axis.ticks = element_blank(),
+         axis.text = element_blank())

```

The t -SNE plot generated by this code is shown in Figure 11. Visually, one of the predominant trends is the clustering of brain tissues reflecting the greater genetic similarity among brain tissues. But there may be other interesting patterns that are revealed more effectively by a matrix factorization.

The **flashier** package implements the *empirical Bayes matrix factorization* (EBMF) framework developed by Wang and Stephens (2021). EBMF is based on the following model of an $n \times p$ data matrix \mathbf{X} :

$$\begin{aligned}
\mathbf{X} &= \mathbf{L}\mathbf{F}' + \mathbf{E} \\
e_{ij} &\sim \mathcal{N}(0, \sigma^2) \\
\ell_{ik} &\sim g_\ell^{(k)} \in \mathcal{G}_\ell \\
f_{jk} &\sim g_f^{(k)} \in \mathcal{G}_f,
\end{aligned} \tag{27}$$

where \mathbf{L} , \mathbf{F} , \mathbf{E} are, respectively, matrices of dimension $n \times K$, $p \times K$ and $n \times p$ storing real-valued elements ℓ_{ik} , f_{jk} , and e_{ij} . The matrices \mathbf{L} and \mathbf{F} form an *approximate low-rank representation* of \mathbf{X} — $\mathbf{X} \approx \mathbf{L}\mathbf{F}^T$ — and this low-rank representation is learned from the data. K specifies the rank of the reduced representation, and is typically set to a positive number much smaller than n and p .

The flexibility of the EBMF framework comes from its ability to accommodate, in principle, any choice of prior family for \mathcal{G}_ℓ and \mathcal{G}_f . As we illustrate below, different choices of prior families can lead to very different factorizations. Some choices closely correspond to existing matrix factorization methods. For example, if \mathcal{G}_ℓ and \mathcal{G}_f are both the families of zero-centered normal priors, then the low-rank representation $\mathbf{L}\mathbf{F}^T$ is expected to be similar to a truncated singular value decomposition (SVD) (Nakajima and Sugiyama 2011). When point-normal prior families are used instead, one obtains empirical Bayes versions of sparse SVD or sparse factor analysis (Engelhardt and Stephens 2010; Yang *et al.* 2014; Witten *et al.* 2009). Thus, EBMF is a highly flexible framework for matrix factorization that includes important previous methods as special cases, but also many new combinations.

Since fitting the EBMF model (27) can be reduced to solving a sequence of EBNM problems (Wang and Stephens 2021), **flashier** leverages **ebnm** for the core model fitting routines. In brief, fitting an EBMF model involves solving an EBNM problem separately for each column of \mathbf{L} and for each column of \mathbf{F} ; the former results in a fitted prior $\hat{g}_\ell^{(k)}$ and posterior estimates of entries ℓ_{ik} , and the latter results in a fitted prior $\hat{g}_f^{(k)}$ and posterior estimates of entries f_{jk} . These EBNM models are repeatedly re-fitted until the priors and posterior estimates converge

to a fixed point. Therefore, fitting an EBMF model can involve solving many hundreds or even many thousands of EBNM problems. Leveraging the efficient EBNM solvers available in **ebnm** makes it possible for **flashier** to tackle large-scale matrix factorization problems.

The **flashier** function `flash()` provides the main interface for fitting EBMF models. The following call to `flash()` fits a matrix factorization to the GTEx data with normal priors on **L** and **F**:

```
R> flash_n <- flash(gtex, ebnm_fn = ebnm_normal, backfit = TRUE)
```

The `ebnm_fn` argument specifies the prior family for **L** and **F**, and accepts any of the prior family functions implemented in the **ebnm** package (e.g., `ebnm_point_normal` or `ebnm_unimodal`; see Table 1 for a near-complete list of prior families). Specifying the number of factors K is not needed because **flashier** automatically tries to determine an appropriate rank by checking whether the addition of new factors substantially improves the fit. (If one prefers a smaller number of factors than what is determined automatically, the maximum number of factors can be adjusted with the `greedy_Kmax` argument.) Here we also turned on backfitting by setting `backfit = TRUE`. This is generally recommended because it improves the quality of the fit (Wang and Stephens 2021), with the caveat that it may make the model fitting too slow for very large data sets. Even with backfitting, the full computation here is very fast; when running this example on a current MacBook Pro, for example, the model fitting is completed in less than one second.

The `plot()` method for "flash" objects can be used to visualize the estimated matrix **L**. Adding color to distinguish among tissues yields an effective visualization that aids interpretation of factors:

```
R> plot(flash_n, include_scree = FALSE, pm_colors = gtex_colors)
```

The plot generated by this call to `plot()` is shown in Figure 12. The first factor sets the “baseline” z -score for each tissue. Other factors appear to capture expected trends: for example, factor 2 picks up a z -score pattern that is more dominant in brain tissues. More tissue-specific patterns are picked up by factor 3, which captures whole blood effects, and factor 6, which captures effects more specific to testis.

SVD and SVD-like matrix factorizations may provide compact approximations of a data matrix, but they are generally known to have poor interpretability. “Sparse” factorizations can produce factors that are much more individually interpretable. In the EBNM framework, a sparse matrix factorization can be achieved by choosing a flexible prior family that better encourages sparsity in **L** and/or **F**. The **flashier** interface makes it straightforward to experiment with different prior families; for example, we can use point-normal priors by simply modifying the `ebnm_fn` argument:

```
> flash_pn <- flash(gtex, ebnm_fn = ebnm_point_normal, backfit = TRUE)
> plot(flash_pn, include_scree = FALSE, pm_colors = gtex_colors)
```

The point-normal priors require estimation of slightly more parameters than the normal priors, but the call to `flash()` is still fast; it took less than 5 seconds to run on our MacBook Pro. This new factorization obtained using point-normal priors is shown in Figure 13. As before, the first factor acts as a “baseline” and the second factor captures z -scores largely specific to

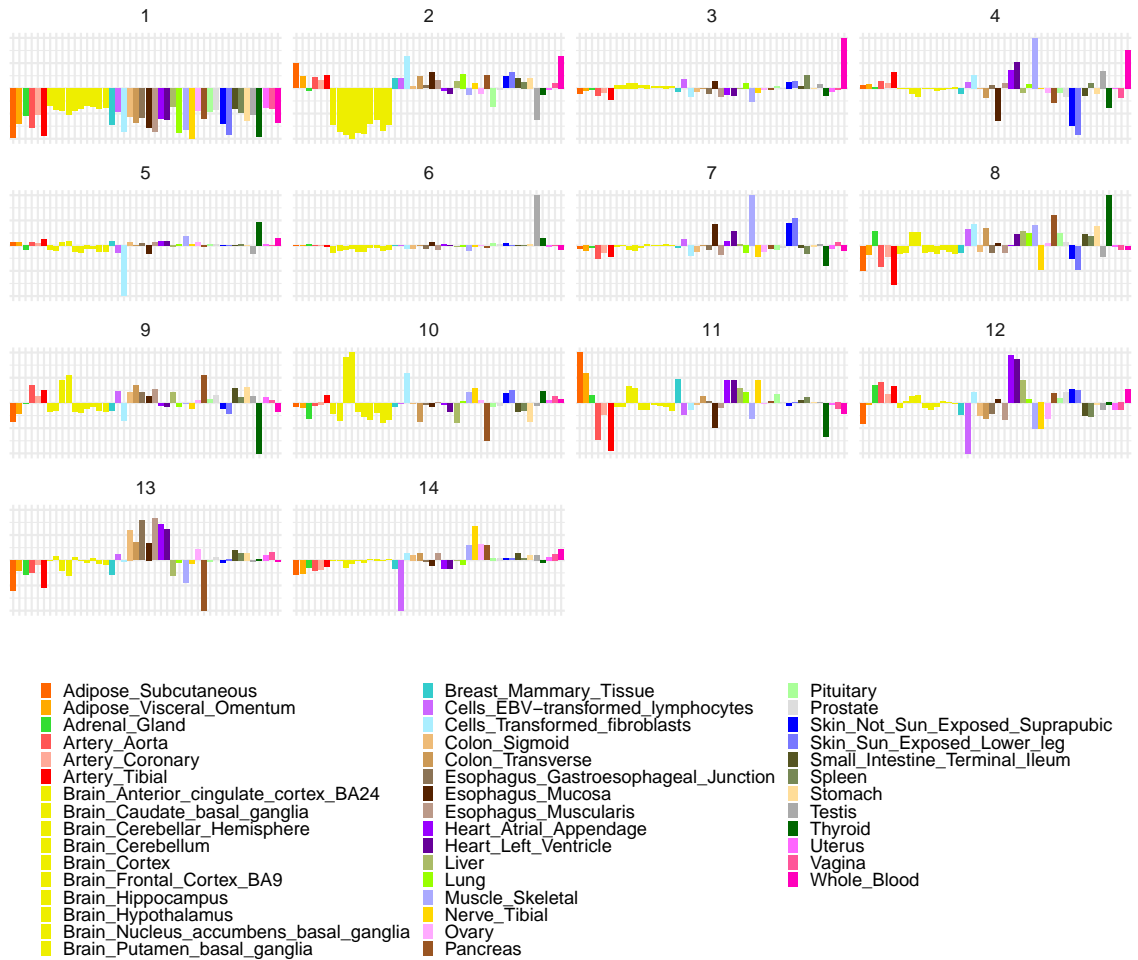


Figure 12: An EBMF model fit to the GTEx data using **flashier**, with normal priors used for elements of \mathbf{L} and \mathbf{F} . Each panel shows the parameter estimates for a column of the \mathbf{F} matrix. The colors used to indicate tissues are the same as in Figure 11. Note that the scale of the y -axis for each plot is not shown because it is largely irrelevant; what matters most is the the sign and relative height of the estimates.

brain tissues. However, there are also some major differences: some factors are much more clearly tissue-specific (e.g., factors 3 and 4 for, respectively, whole blood and testis); other patterns include cerebellar-specific patterns (factor 9) and heart-specific patterns (factor 12). These same patterns are also captured in the matrix factorization with normal priors, but they often appear in combination with other patterns in unintuitive ways.

Another matrix factorization approach that has been recently proposed is *semi-nonnegative matrix factorization* (Ding *et al.* 2010; Wang *et al.* 2019; He *et al.* 2020), in which the elements of either \mathbf{L} or \mathbf{F} (but not both) are constrained to be nonnegative. Supposing that \mathbf{L} is constrained to be nonnegative, the elements $\ell_{ik} \geq 0$ can be viewed as “weights” or “memberships,” and each row of \mathbf{X} is then interpretable as a weighted combination of factors: $x_i \approx \sum_{k=1}^K \ell_{ik} f_{\cdot k}$.

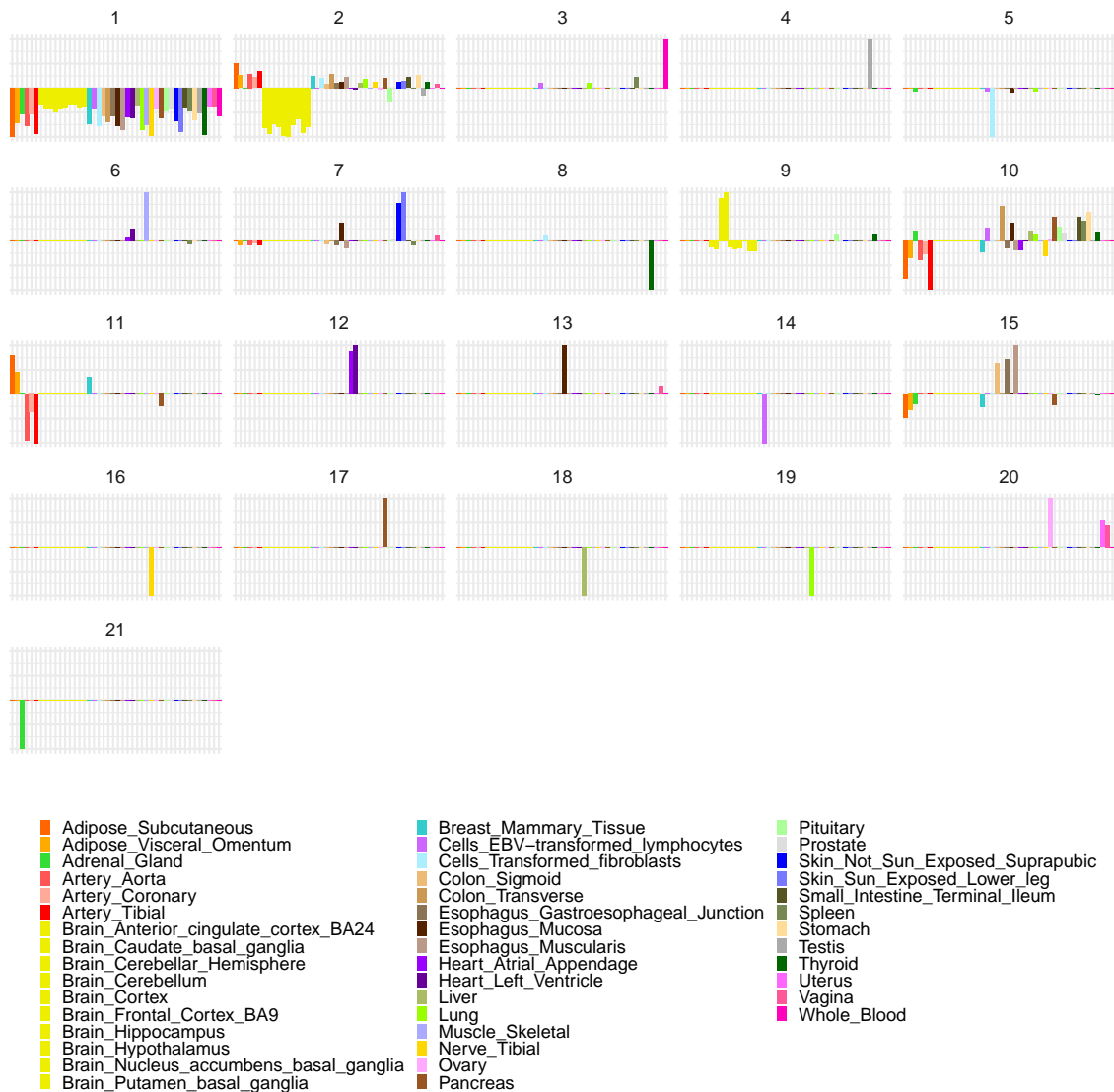


Figure 13: An EBMF model fit to the GTEx data using **flashier**, with point-normal priors used for elements of \mathbf{L} and \mathbf{F} .

To obtain a semi-nonnegative matrix factorization via **flashier**, one need only choose appropriate prior families. Here we use point-normal priors for \mathbf{L} and point-exponential priors for \mathbf{F} ; thus we combine the benefits of both semi-nonnegative and sparse matrix factorization. In **flashier**, we can specify different priors for \mathbf{L} and \mathbf{F} by setting the `ebnm_fn` argument to be a list in which the first element is the prior family for \mathbf{L} and the second the prior family for \mathbf{F} :

```
R> flash_snn <- flash(gtex,
+                   ebnm_fn = c(ebnm_point_normal, ebnm_point_exponential),
+                   backfit = TRUE)
R> plot(flash_snn, include_screen = FALSE, pm_colors = gtex_colors)
```

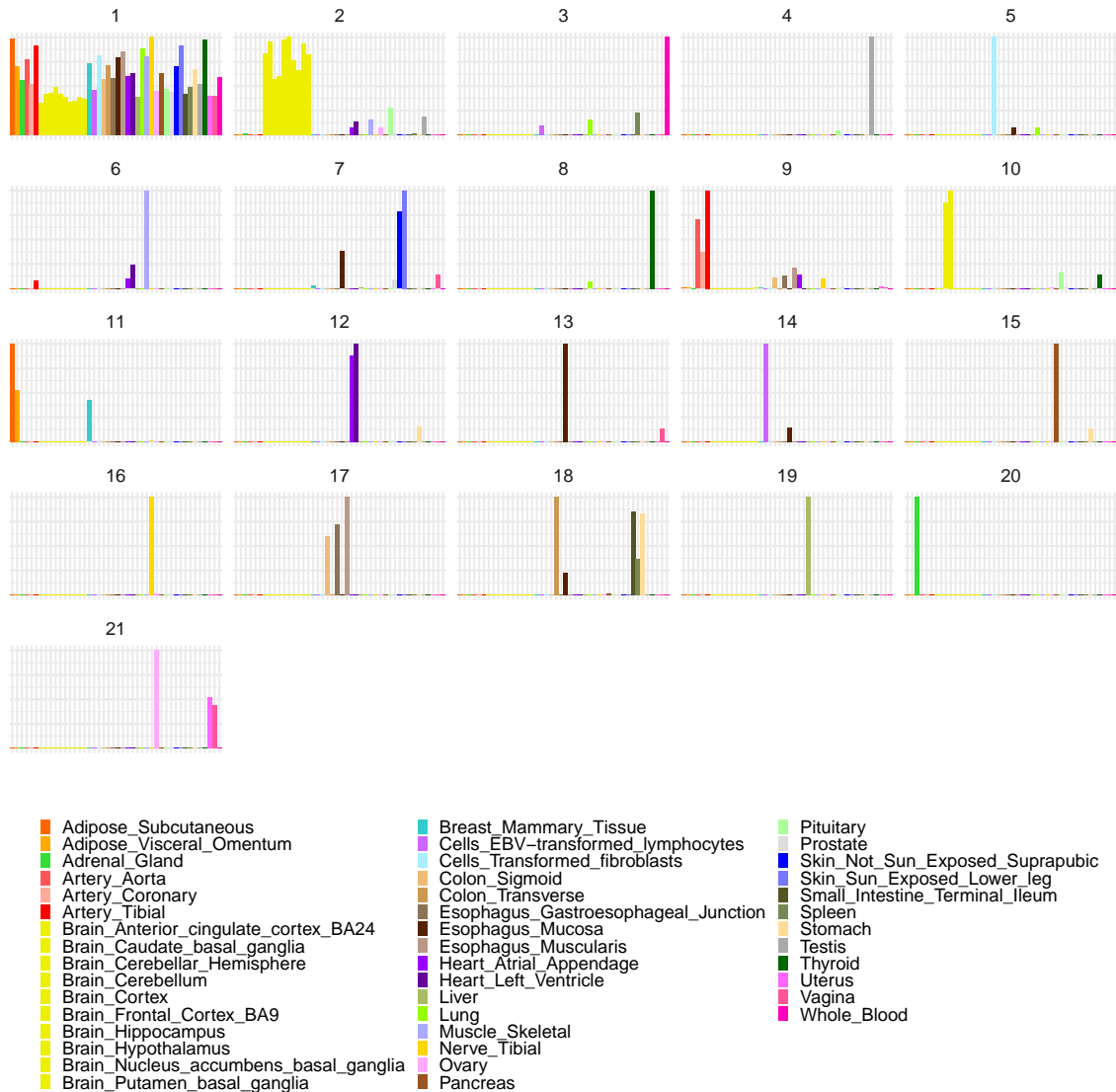


Figure 14: An EBMF model fit to the GTEx data using **flashier**, with point-normal priors used for elements of \mathbf{L} and point-exponential priors for elements of \mathbf{F} .

This code returned results in less than 3 seconds on our MacBook Pro.

The semi-nonnegative factorization generated by this `flash()` call is shown in Figure 14. The result is in many ways strikingly similar to the sparse factorization obtained using point-normal priors (Figure 13). In some cases, the same tissue-specific effects are recovered, up to a difference in signs (e.g., factor 5 for fibroblasts and factor 8 for thyroid). But the semi-nonnegative factorization identifies factors that are arguably more intuitive; for example, point-normal factor 10, which combines artery and adipose tissues (Figure 13), is split into two factors in the semi-nonnegative factorization (factor 9 for artery and factor 11 for adipose tissue).

The **flashier** package has many more options which we did not explore here, including other choices of prior family, different options for estimating the variances of the residuals \mathbf{E} , and options for fine-tuning the model fitting to improve the speed and quality of EBMF model fits for larger data sets.

7. Summary

The **ebnm** package provides a comprehensive toolkit for solving the empirical Bayes normal means problem under different prior assumptions. In many situations — including in our analyses of baseball statistics and genetics data — the “best” choice of prior family may not be known in advance. The **ebnm** package is especially well-suited to handling such situations by providing a large set of prior families to choose from (Table 1), and an interface that allows for convenient comparison of the different prior families. When deciding which prior family to proceed with, our general recommendation is to weigh prior assumptions about the data against empirical measures of fit.

References

- Bhadra A, Datta J, Polson NG, Willard B (2019). “Lasso meets horseshoe: a survey.” *Statistical Science*, **34**(3), 405–427.
- Box EP, Tiao GC (1965). “Multiparameter problems from a Bayesian point of view.” *Annals of Mathematical Statistics*, **36**(5), 1468–1482.
- Brown LD (2008). “In-season prediction of batting averages: a field test of empirical Bayes and Bayes methodologies.” *Annals of Applied Statistics*, **2**(1), 113–152.
- Carvalho CM, Polson NG, Scott JG (2010). “The horseshoe estimator for sparse signals.” *Biometrika*, **97**(2), 465–480.
- Chen MH, Shao QM (1999). “Monte Carlo estimation of Bayesian credible and HPD intervals.” *Journal of Computational and Graphical Statistics*, **8**(1), 69–92.
- Clyde M, George EI (2000). “Flexible empirical Bayes estimation for wavelets.” *Journal of the Royal Statistical Society, Series B*, **62**(4), 681–698.
- Dicker LH, Zhao SD (2016). “High-dimensional classification via nonparametric empirical Bayes and maximum likelihood inference.” *Biometrika*, **103**(1), 21–34.
- Ding CH, Li T, Jordan MI (2010). “Convex and semi-nonnegative matrix factorizations.” *IEEE Transactions on Pattern Analysis and Machine Intelligence*, **32**(1), 45–55.
- Efron B (2010). *Large-scale inference: empirical Bayes methods for estimation, testing, and prediction*, volume 1 of *Institute of Mathematical Statistics Monographs*. Cambridge University Press, Cambridge, UK.
- Efron B, Morris C (1972). “Limiting the risk of Bayes and empirical Bayes estimators—Part II: the empirical Bayes case.” *Journal of the American Statistical Association*, **67**(337), 130–139.

- Efron B, Morris C (1973). “Stein’s estimation rule and its competitors—an empirical Bayes approach.” *Journal of the American Statistical Association*, **68**(341), 117–130.
- Engelhardt BE, Stephens M (2010). “Analysis of population structure: A unifying framework and novel methods based on sparse factor analysis.” *PLOS Genetics*, **6**(9), 1–12.
- FanGraphs (2023). “Guts!” URL <https://www.fangraphs.com/guts.aspx>.
- Geyer CJ (2020). *trust: trust region optimization*. R package version 0.1-8, URL <https://CRAN.R-project.org/package=trust>.
- Gu J, Koenker R (2017). “Empirical Bayesball remixed: empirical Bayes methods for longitudinal data.” *Journal of Applied Econometrics*, **32**(3), 575–599.
- Hastie T, Tibshirani R, Friedman J (2009). *The Elements of Statistical Learning*. second edition. Springer, New York, NY.
- He Y, Chhetri SB, Arvanitis M, Srinivasan K, Aguet F, Ardlie KG, Barbeira AN, Bonazzola R, Im HK, GTEx Consortium, Brown CD, Battle A (2020). “sn-spMF: matrix factorization informs tissue-specific genetic regulation of gene expression.” *Genome Biology*, **21**, 235.
- James W, Stein C (1961). “Estimation with quadratic loss.” In *Berkeley Symposium on Mathematical Statistics and Probability, 1961*, pp. 361–379. University of California Press, Berkeley, CA.
- Jiang W, Zhang CH (2009). “General maximum likelihood empirical Bayes estimation of normal means.” *Annals of Statistics*, **37**(4), 1647–1684.
- Jiang W, Zhang CH (2010). “Empirical Bayes in-season prediction of baseball batting averages.” In *Borrowing strength: theory powering applications—a Festschrift for Lawrence D. Brown*, volume 6 of *Institute of Mathematical Statistics Collections*, pp. 263–273. Institute of Mathematical Statistics, Beachwood, OH.
- Johnstone I (2019). “Gaussian estimation: sequence and wavelet models.” URL <http://www-stat.stanford.edu/~imj>.
- Johnstone I, Silverman BW (2005a). “EbayesThresh: R programs for empirical Bayes thresholding.” *Journal of Statistical Software*, **12**(8), 1–38.
- Johnstone IM, Silverman BW (2004). “Needles and straw in haystacks: empirical Bayes estimates of possibly sparse sequences.” *Annals of Statistics*, **32**(4), 1594–1649.
- Johnstone IM, Silverman BW (2005b). “Empirical Bayes selection of wavelet thresholds.” *Annals of Statistics*, **33**(4), 1700–1752.
- Judge J (2019). “Entirely beyond WOWY: a breakdown of DRC+.” *Baseball Prospectus*. URL <https://www.baseballprospectus.com/news/article/48293/entirely-beyond-wowy-a-breakdown-of-drc/>.
- Kiefer J, Wolfowitz J (1956). “Consistency of the maximum likelihood estimator in the presence of infinitely many incidental parameters.” *Annals of Mathematical Statistics*, **27**(4), 887–906.

- Kim Y, Carbonetto P, Stephens M, Anitescu M (2020). “A fast algorithm for maximum likelihood estimation of mixture proportions using sequential quadratic programming.” *Journal of Computational and Graphical Statistics*, **29**(2), 261–273.
- Kim Y, Wang W, Carbonetto P, Stephens M (2022). “A flexible empirical Bayes approach to multiple linear regression and connections with penalized regression.” *arXiv*, **2208.10910**.
- Koenker R (2017). “Bayesian deconvolution: an R vinaigrette.” *Technical report*, cemmap working paper No. CWP38/17. URL <http://hdl.handle.net/10419/189756>.
- Koenker R, Gu J (2017). “REBayes: an R Package for empirical Bayes mixture methods.” *Journal of Statistical Software*, **82**(8), 1–26.
- Koenker R, Mizera I (2014). “Convex optimization, shape constraints, compound decisions, and empirical Bayes rules.” *Journal of the American Statistical Association*, **109**(506), 674–685.
- Krijthe JH (2015). *Rtsne: T-distributed stochastic neighbor embedding using Barnes-Hut implementation*. R package version 0.15, URL <https://github.com/jkrijthe/Rtsne>.
- Laird N (1978). “Nonparametric maximum likelihood estimation of a mixing distribution.” *Journal of the American Statistical Association*, **73**(364), 805–811.
- Lindsay BG (1983). “The geometry of mixture likelihoods: a general theory.” *Annals of Statistics*, **11**(1), 86–94.
- Liu Y, Carbonetto P, Willwerscheid J, Oakes SA, MacLeod KF, Stephens M (2023). “Dissecting tumor transcriptional heterogeneity from single-cell RNA-seq data by generalized binary covariance decomposition.” *bioRxiv*.
- Lonsdale J, Thomas J, Salvatore M, *et al.* (2013). “The Genotype-Tissue Expression (GTEx) project.” *Nature Genetics*, **45**(6), 580–585.
- Love MI, Huber W, Anders S (2014). “Moderated estimation of fold change and dispersion for RNA-seq data with DESeq2.” *Genome Biology*, **15**, 550.
- Mersmann O (2019). *microbenchmark: accurate timing functions*. R package version 1.4.9, URL <https://CRAN.R-project.org/package=microbenchmark>.
- Morris CN (1983). “Parametric empirical Bayes inference: theory and applications.” *Journal of the American Statistical Association*, **78**(381), 47–55.
- MOSEK ApS (2019). *Rmosek: the R to MOSEK optimization interface*. R package version 9.1.0, URL <http://www.mosek.com/>.
- Mukherjee S, Sen B, Sen S (2023). “A mean field approach to empirical Bayes estimation in high-dimensional linear regression.” *arXiv*, **2309.16843**.
- Nakajima S, Sugiyama M (2011). “Theoretical analysis of Bayesian matrix factorization.” *Journal of Machine Learning Research*, **12**, 2583–2648.
- Narasimhan B, Efron B (2020). “deconvolveR: a g-modeling program for deconvolution and empirical Bayes Estimation.” *Journal of Statistical Software*, **94**(11), 1–20.

- Robbins H (1951). “Asymptotically subminimax solutions of compound statistical decision problems.” In *Proceedings of the Second Berkeley Symposium on Mathematical Statistics and Probability, 1951, vol. II*, pp. 131–149. University of California Press, Berkeley and Los Angeles, CA.
- Robbins H (1956). “An empirical Bayes approach to statistics.” In *Proceedings of the Third Berkeley Symposium on Mathematical Statistics and Probability, 1956, vol. I*, pp. 157–163. University of California Press, Berkeley and Los Angeles, CA.
- Robinson D (2017). “Introduction to empirical Bayes: examples from baseball statistics.” URL <https://github.com/dgrtwo/empirical-bayes-book>.
- Sharpe S (2019). “An introduction to expected weighted on-base average (xwOBA).” *MLB Technology Blog*. URL <https://technology.mlblogs.com/an-introduction-to-expected-weighted-on-base-average-xwoba-29d6070ba52b>.
- Silverman BW, Evers L, Xu K, Carbonetto P, Stephens M (2017). *EbayesThresh: empirical Bayes thresholding and related methods*. R package version 1.4-12, URL <https://CRAN.R-project.org/package=EbayesThresh>.
- Stein C (1956). “Inadmissibility of the usual estimator for the mean of a multivariate normal distribution.” In *Proceedings of the Third Berkeley Symposium on Mathematical Statistics and Probability, 1954–1955, vol. I*, pp. 197–206. University of California Press, Berkeley and Los Angeles, CA.
- Stephens M (2017). “False discovery rates: a new deal.” *Biostatistics*, **18**(2), 275–294.
- Stephens M, Carbonetto P, Gerard D, Lu M, Sun L, Willwerscheid J, Xiao N (2023). *ashr: methods for adaptive shrinkage, using empirical Bayes*. R package version 2.2-63, URL <https://CRAN.R-project.org/package=ashr>.
- Sun L (2020). *Topics on empirical Bayes normal means*. Ph.D. thesis, University of Chicago, Chicago, IL.
- Tango T, Lichtman M, Dolphin A (2006). *The book: Playing the percentages in baseball*. TMA Press.
- Urbut SM, Wang G, Carbonetto P, Stephens M (2019). “Flexible statistical methods for estimating and testing effects in genomic studies with multiple conditions.” *Nature Genetics*, **51**, 187–195.
- Van der Maaten L (2014). “Accelerating t-SNE using tree-based algorithms.” *Journal of Machine Learning Research*, **15**, 3221–3245.
- Van der Maaten L, Hinton G (2008). “Visualizing data using t-SNE.” *Journal of machine learning research*, **9**(11).
- Van der Pas S, Scott J, Chakraborty A, Bhattacharya A (2019). *horseshoe: implementation of the horseshoe prior*. R package version 0.2.0, URL <https://CRAN.R-project.org/package=horseshoe>.

- Wang M, Fischer J, Song YS (2019). “Three-way clustering of multi-tissue multi-individual gene expression data using semi-nonnegative tensor decomposition.” *Annals of Applied Statistics*, **13**(2), 1103–1127.
- Wang W, Stephens M (2021). “Empirical Bayes matrix factorization.” *Journal of Machine Learning Research*, **22**(120), 1–40.
- Wickham H (2016). *ggplot2: elegant graphics for data analysis*. Springer-Verlag, New York, NY.
- Willwerscheid J (2021). *Empirical Bayes matrix factorization: methods and applications*. Ph.D. thesis, University of Chicago, Chicago, IL.
- Willwerscheid J, Carbonetto P, Wang W, Stephens M (2023). *flashier: empirical Bayes matrix factorization*. R package version 1.0.0, URL <https://github.com/willwerscheid/flashier>.
- Witten DM, Tibshirani R, Hastie T (2009). “A penalized matrix decomposition, with applications to sparse principal components and canonical correlation analysis.” *Biostatistics*, **10**(3), 515–534.
- Yang D, Ma Z, Buja A (2014). “A sparse singular value decomposition method for high-dimensional data.” *Journal of Computational and Graphical Statistics*, **23**(4), 923–942.
- Zhang Y, Cui Y, Sen B, Toh KC (2022). “On efficient and scalable computation of the nonparametric maximum likelihood estimator in mixture models.” *arXiv*.
- Zhu A, Ibrahim JG, Love MI (2019). “Heavy-tailed prior distributions for sequence count data: removing the noise and preserving large differences.” *Bioinformatics*, **35**(12), 2084–2092.

A. Supplementary benchmarking results

A.1. Optimization methods for parametric families

We first compare the performance of six optimization methods, all of which are implemented in **ebnm** via parameter `optmethod`. In each case, parameters are transformed so that the optimization problem is unconstrained (specifically, a log transformation is used for scale parameters, which are constrained to be nonnegative, while a logit transformation is used for mixture proportions, which are constrained to lie between zero and one).

Three choices of `optmethod` call into function `nlm()`, a Newton-type algorithm included in the base **stats** package. Gradient and Hessian functions can be provided; if they are not, `nlm()` estimates them numerically. Option `optmethod = "nlm"` provides both the gradient and Hessian functions; `optmethod = "nohess_nlm"` provides the gradient but not the Hessian; `optmethod = "nograd_nlm"` provides neither. Options `optmethod = "lbfgsb"` and `optmethod = "nograd_lbfgsb"` call into function `optim()`, also in the **stats** package, with argument `method = "L-BFGS-B"`. The former provides the gradient function; the second does not. By definition, L-BFGS-B does not accept a Hessian. Finally, `optmethod = "trust"` calls

into function `trust()`, a trust-region algorithm implemented in the `trust` package (Geyer 2020). Since `trust()` requires both a gradient and Hessian function, there is only one corresponding `optmethod`. In sum, then, there are two methods that use both gradients and Hessians ("`nlm`" and "`trust`"); two that use only gradients ("`nohess_nlm`" and "`lbfgsb`"); and two that estimate all derivatives numerically ("`nograd_nlm`" and "`nograd_lbfgsb`").

For both `ebnm_point_normal()` and `ebnm_point_laplace()`, we ran tests for $2 \times 3 \times 2 \times 3 = 36$ scenarios:

- The mode is either fixed at zero via argument `mode = 0` or estimated (via `mode = "estimate"`).
- The data-generating prior distribution g is: i) a true member of the prior family, $\pi_0 \delta_\mu + (1 - \pi_0)N(\mu, a^2)$ or $\pi_0 \delta_\mu + (1 - \pi_0)\text{Laplace}(\mu, a)$, with $\pi_0 \sim \text{Beta}(10, 2)$, $a \sim \text{Gamma}(4, 1)$, and either $\mu = 0$ or $\mu \sim \text{Unif}[-10, 10]$; ii) the null distribution δ_0 ; or iii) a distribution not in the prior family, so that \mathcal{G} is misspecified. When `mode = 0`, the misspecified prior is a point-normal prior as above but with $\mu \sim \text{Unif}[-10, 10]$; when `mode = "estimate"`, the misspecified prior is the point- t_5 distribution $\pi_0 \delta_0 + (1 - \pi_0)t_5(0, a)$, with π_0 and a distributed as above.
- The $N(0, s_i^2)$ noise added to the true means $\theta_i \sim g$ is either homoskedastic, with $s_i = 1$ for all i , or heteroskedastic, with $s_i^2 - 1 \sim \text{Exp}(1)$.
- The number of observations n is 1000, 10000, or 100000.

For each scenario, we ran $10^6/n$ simulations (so, depending on n , 1000, 100, or 10 simulations) and compared runtimes using package `microbenchmark` (Mersmann 2019). All experiments were performed on a 2021 MacBook Pro with an Apple M1 Max processor and 64 GB of unified memory. Results are displayed in Figures 15 and 16.

In general, the methods that supplied the gradient function outperformed the methods that required all derivatives to be estimated numerically. Timing was similar among the four methods that do supply the gradient. However, method "`lbfgsb`" failed to converge in several of the `prior_null` simulations (in some scenarios, up to 7% of simulations resulted in an error). Further, the methods that supply Hessians ("`nlm`" and "`trust`") occasionally struggled when the data-generating prior was the null distribution δ_0 . We thus recommend the default setting `optmethod = "nohess_nlm"`.

A.2. Comparisons with existing packages

Next we compare the performance of `ebnm` against three packages with directly comparable functions: function `ebnm_point_laplace()` is closely related to function `ebayesthresh()` in the `EbayesThresh` package (Silverman *et al.* 2017); function `ebnm_normal_scale_mixture()` is modelled on function `ash()` in the `ashr` package (with option `mixcompdist = "normal"`; Stephens *et al.* (2023)) but is implemented in a much simpler manner; and function `ebnm_npmle()` performs a similar task to function `GLmix()` in the `REBayes` package (Koenker and Gu 2017).

We ran tests for the same scenarios as Section A.1, with the difference that the mode is always fixed at zero (mode estimation is not possible with `EbayesThresh`). Further, since

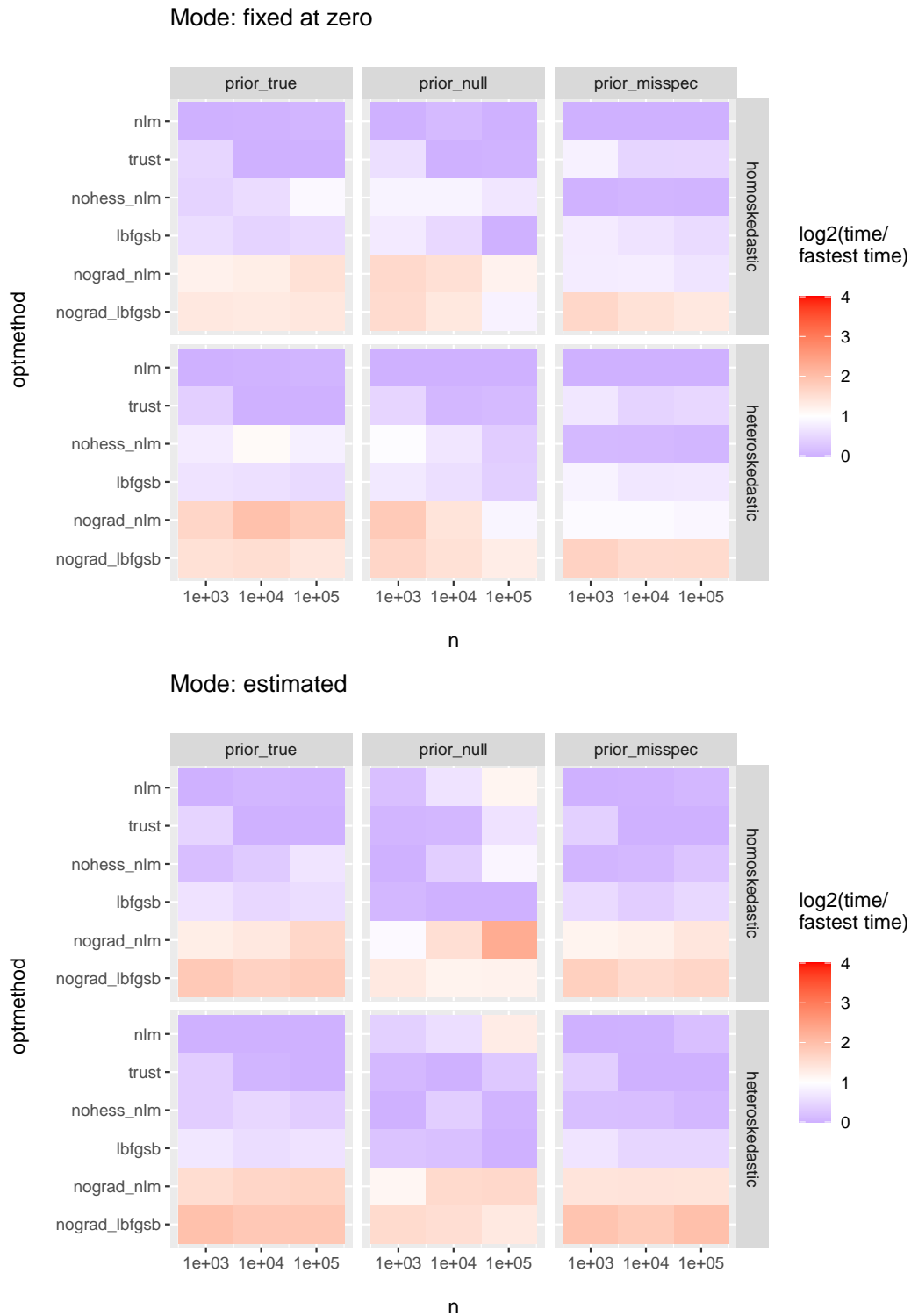


Figure 15: Timing comparisons for `ebnm_point_normal()`. Tests in the top figure fix the mode at zero (by setting argument `mode = 0`) while those in the bottom estimate the mode (by setting `mode = "estimate"`). Different columns correspond to different data-generating priors: a true member of the point-normal prior family; the null distribution δ_0 ; or a distribution from outside the prior family. Different rows correspond to different noise models, with the noise added to the “true” observations either homoskedastic (with $s_i = 1$ for all i) or heteroskedastic (with $s_i^2 - 1 \sim \text{Exp}(1)$). Plotted is the time as a multiple of the fastest time for a given combination of mode, prior, noise, and value of n . Shades of blue indicate optimization methods that are within a factor of 2 of the fastest method for that mode, prior, noise, and value of n , while shades of red indicate slower methods.

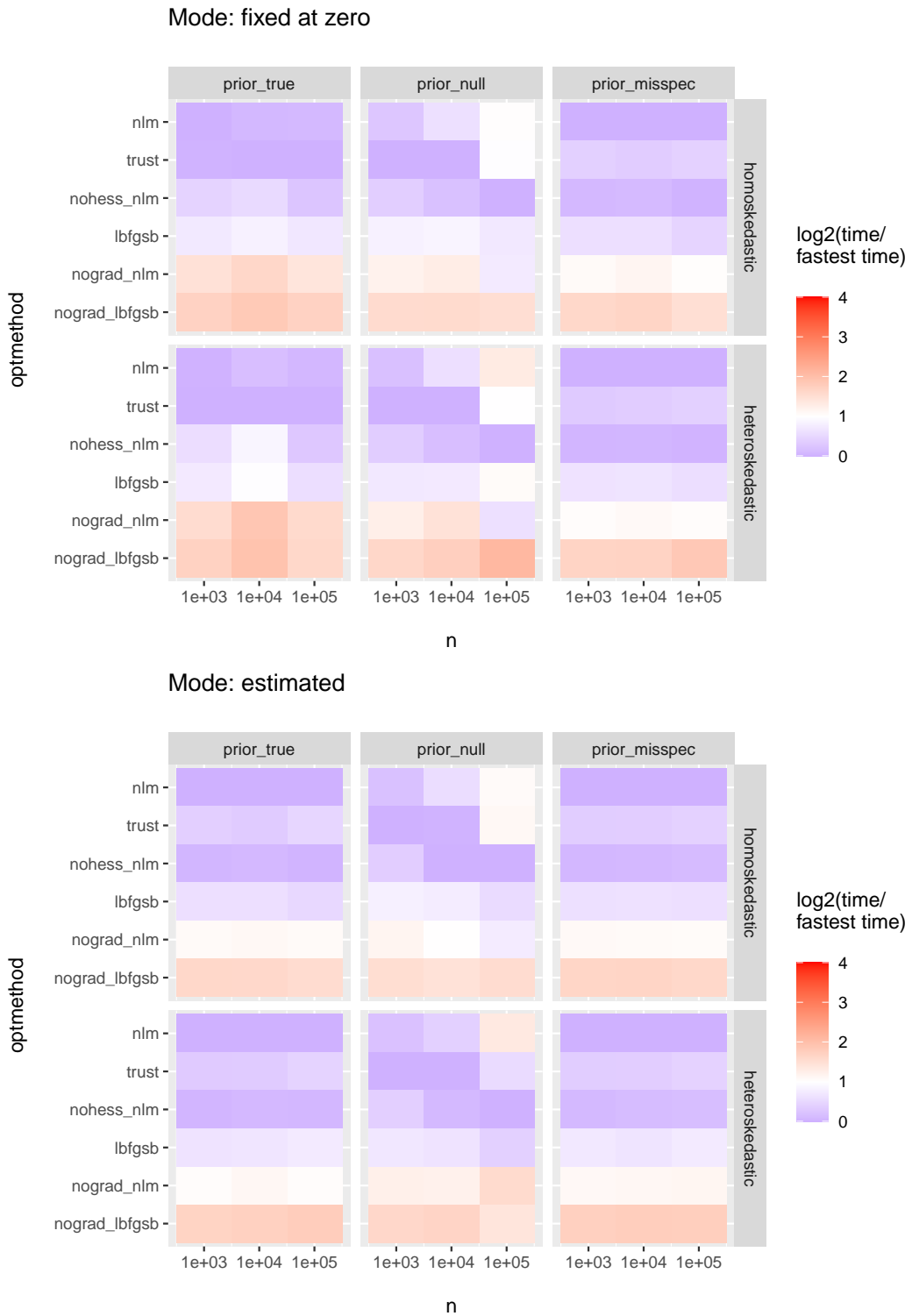


Figure 16: Timing comparisons for `ebnm_point_laplace()`. See Figure 15 caption and text for details.

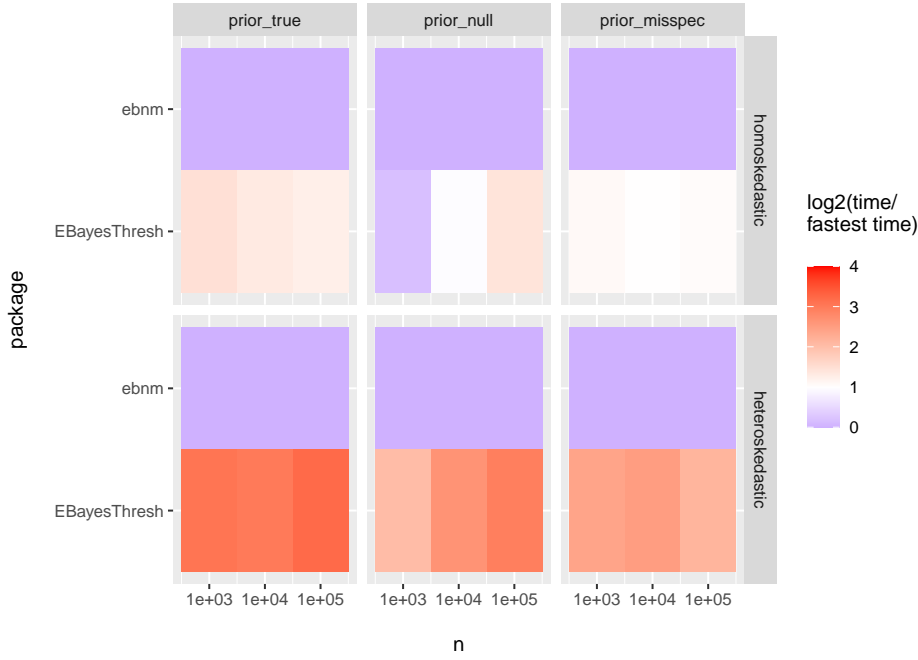


Figure 17: Timing comparisons: `ebnm_point_laplace` vs. `ebayesthresh`. See Figure 15 caption and text for details.

it is not possible to “misspecify” the prior for the family of all distributions $\mathcal{G}_{\text{npmlc}}$, we only considered a single data-generating distribution (the point-Laplace), but we varied the number of grid points (mixture components) from 10 to 300. The number of simulations, microbenchmark settings, and hardware were as described in Section A.1. We set parameters to make outputs as similar as possible. For `EBayesThresh`, we set `threshrule = "mean"` and `universalthresh = FALSE`; for `ash()`, we set `prior = "uniform"`. Results are given in Figures 17–19.

In some scenarios, `EBayesThresh` was nearly as fast as `ebnm_point_laplace()`, but in others it was outperformed by a full order of magnitude. Further, `ebnm` regularly found significantly better solutions than `EBayesThresh` (in terms of the final objective attained) except when the data-generating prior was the null distribution, in which cases the packages found solutions of similar quality.

When the number of observations was small, `ebnm` was faster than `ashr` by a factor of around 2 to 4, but `ashr` performed comparably to `ebnm_normal_scale_mixture()` for large problems. Results in the comparison between `ebnm_npmlc()` and `REBayes` were mixed. `ebnm` was regularly faster when the number of mixture components was small (fewer than 100), while `REBayes` was consistently faster when a dense grid was used (more than 100 components). According to the theory developed in Willwerscheid (2021), 100 components should be “good enough” for homoskedastic observations when

$$n^{1/4} \left(\frac{\text{range}(x)}{s} \right) \leq 400. \quad (28)$$

For example, if the number of observations $n = 10^4$, then 100 components should suffice as

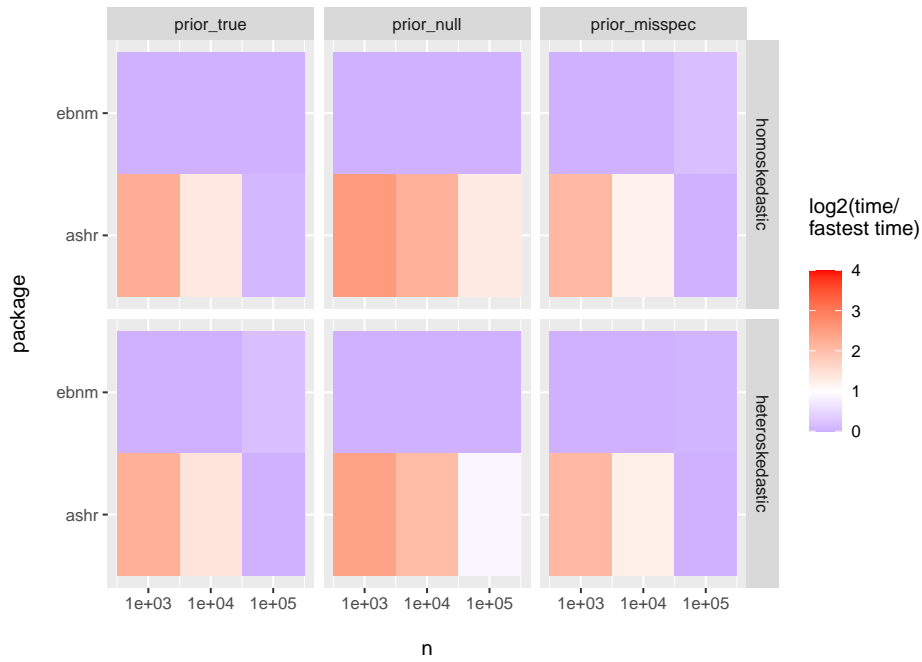


Figure 18: Timing comparisons: `ebnm_normal_scale_mixture` vs. `ashr`. See Figure 15 caption and text for details.

long as the studentized range

$$\frac{\max(x) - \min(x)}{s} \leq 40. \quad (29)$$

Affiliation:

Jason Willwerscheid
 Department of Mathematics and Computer Science
 Providence College
 Providence, Rhode Island, United States of America
 E-mail: jwillwer@providence.edu

Peter Carbonetto
 Department of Human Genetics and the
 Research Computing Center
 University of Chicago
 Chicago, Illinois, United States of America
 E-mail: pcarbo@uchicago.edu

Matthew Stephens
 Departments of Statistics and Human Genetics
 University of Chicago

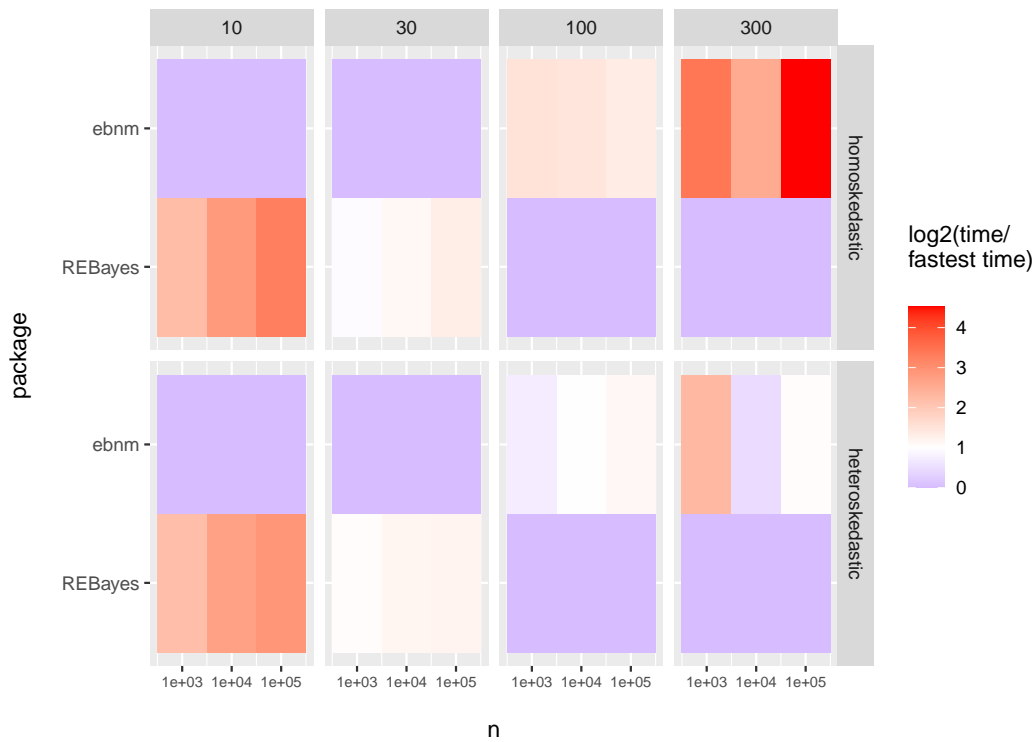


Figure 19: Timing comparisons: `ebnm_npmle` vs. `REBayes`. Column headers indicate the number of grid points (mixture components) that were used to estimate the NPMLE. All simulations were from a point-Laplace distribution; the noise models (homoskedastic and heteroskedastic) are as above (see Figure 15 caption for details).

Chicago, Illinois, United States of America

E-mail: mstephens@uchicago.edu